Technical University Of Crete
School of Electronic And Computer Engeeniring

"Video Traffic Modeling by Exploiting Inter-Frame Correlation Coefficients"

Athina Kalampogia

Thesis committee

Advisor: Associate Professor Polychronis Koutsakis

Professor Michael Paterakis

Professor Michael Zervakis

Chania, September 2014

ACKNOWLEDGEMENTS

There are a lot of people I wish to thank for helping me complete my Thesis.

First of all, I would like to thank my advisor, Polychronis Koutsakis for believing in me and making me believe in myself, for the opportunity he gave me to work with him and for all the guidance and support from the beginning of my thesis until the end.

I would like to thank Professors Michael Paterakis and Michael Zervakis for their participation in the examination committee.

Finally, I would like to thank my family that always support me and help me succeed in my goals and of course my friends for being there when I needed them.

Working on my thesis was the most interesting and exciting experience in my academic life so far. Although there were tough times, completing this work gave me self-confidence and I wish to continue my studies in this field of research.

September 2014,

Kalampogia Athina

ABSTRACT

The explosive growth of multimedia applications renders the efficiency network resource allocation a problem of major importance. The burstiness of video traffic, in particular, calls for innovative ideas that will help prevent significant packet losses that could cause bad Quality of Service (QoS) and Quality of Experience (QoE) to users. In this work, we analyze the traffic characteristics of H.264 encoded video and we propose and evaluate the accuracy of a H.264 video traffic model that predicts the size of B-frames. B-frame prediction can be used in order to reduce bandwidth requirements and smoothen the encoded video stream, by selective B-frame dropping, when the model predicts larger B-frame traffic than the network can handle. We implement three prediction models and after comparing them against each other we conclude which model offers the highest accuracy. It will be shown that our approach clearly outperforms another model recently proposed in the literature, and provides a highly accurate prediction for a wide variety of video traces with different GOP patterns and different qualities. We also show that the third implemented model, which in a previous work in the literature was shown to underperform for MPEG-4 traffic, also produces highly accurate results for H.264 traces.

TABLE OF CONTENTS

List of Table and Figures

Tables

FIGURES

CHAPTER 1: INTRODUCTION

1.1 Introduction

As video services are expected to occupy an overwhelming percentage of the total network traffic in next generation wired and wireless networks, it becomes all the more necessary to optimize the way in which bandwidth is allocated. The network should always be able to provide the quality of service (QoS) requirements of the video traffic. Hence, the optimization should take place without causing loss of packets that affects the quality of the video. Unfortunately, the latest compression standards present high bit rate variability which makes the efficient allocation of bandwidth for the video even harder to achieve. There are two basic problems: if we choose to reduce the bandwidth offered for the transmission there is the possibility of losing packets that are crucial for the quality of the video. On the other hand, if we constantly overallocate bandwidth to handle possible video traffic bursts, we will face the problem of bandwidth wastage.

In this work, we focused on the H.264 video compression standard, which is a video standardization project of the ITU-T Video Coding Experts Group (VCEG) and the ISO/IEC Moving Picture Experts Group (MPEG). It currently is one of the most commonly used video coding standards as it covers a huge range of applications like videoconferencing, mobile services, and HD video storage [1]. There are two basic structural features that common H.264 encoders share: the three types of frames (I, P, B) they generate and the pattern in which these frames are generated.

I-frames are completely self-referential and don't use information from any other frames. They provide a point of access to the compressed video data. I-frames are the largest among the 3 types of frames but the least efficient from a compression perspective. P-frames are "predicted" frames. When producing a P-frame, the encoder can look backwards to previous I or P-frames for redundant picture information. P-frames are smaller than the I-frames [2]. B-frames are bi-directionally predicted frames. This means that when producing B-frames, the encoder can look both forwards and backwards for redundant picture information. This makes B-frames the most efficient of the three.

The encoders of H.264 use a fixed Group-of-Pictures (GOP) pattern when compressing a video sequence. There are two variables that define this pattern: N which indicates the distance between I-frames and M that indicates the distance between P-frames. The values of those variables vary depending on the required video quality and the transmission rate [3].

The subject of video traffic modeling has been widely studied in the literature. An accurate model of the expected video traffic will allow network administrators to make better estimates of the bandwidth that is required for the QoS and quality of the experience (QoE) of their customers. The approaches that have been used in the literature include first-order autoregressive (AR) models [4], discrete AR (DAR) models [5,6], Markov renewal processes (MRP) [7], finite-state Markov chain [8,9], and Gamma–beta-auto-regression (GBAR) models [10,11]. The GBAR model, being an autoregressive model with Gamma-distributed marginals and geometric autocorrelation, “captures” data-rate dynamics of VBR video conferences well. In [12], various differences in successive video frame sizes of VBR video traffic were investigated, while in [13] packet generation intervals, at various levels of video activity, were studied. In [6, 14] the authors show that H.261 videoconference sequences generated by different hardware coders, using different coding algorithms, have gamma marginal distributions (this result was also employed by [15], which proposes an Autoregressive Model of order one for sequences of H. 261 encoding) and use this result to build a Discrete Autoregressive (DAR) model of order one, which works well when several sources are multiplexed.

As analyzed in [16], all the video modeling studies presented above can be classified into two categories: (a) data-rate model, and (b) frame-size models. In a data-rate model, only the rate at which data are arriving at a link is generated for performance prediction purposes. Almost all models, including AR, DAR, MRP, MRP TES and the GBAR model, fall under this category. These models achieve good and often very good results in predicting average packet-loss probability and buffer overflowing probability. However, they have the shortcoming of failing to identify such details as the percentage of frames affected, as even a small rate of data loss involving I frames may affect the perceptual quality of the received video significantly, but the same amount of data loss in B frames would have far less impact. In a frame-size model, sizes of individual MPEG frames are generated, and hence, data-rate information can be obtained from the frame-size information.

An important feature of common H.264 encoders is the manner in which frame types are generated. Typical encoders use several group-of-pictures (GOP) patterns when compressing video sequences; the GOP pattern specifies the number and temporal order of P and B frames between two successive I frames. A GOP pattern is defined by the distance N between I frames and the distance M between P frames.

Usually, in an H.264 GOP there are more B-frames than P or I-frames which leads to B-frames occupying the largest percentage of bandwidth. Comparing the three types of frames and the problem that the loss of each can cause, the loss of B-frames is less harmful than the loss of any other type of frame. This is due to the fact that B-frames use only the differences between the current frame and both the previous and following frames to specify their content, so their loss causes motion artifacts that the human eye has difficulty to understand unless there is a high loss rate. On the other hand, the loss of I-frames or P-frames can cause image distortion that is observable even in the case of low loss rate. Therefore, in order to reduce bit rate variability and have a smoother video bit stream it would be very beneficial for network administrators to be able to predict the volume of traffic and, in case the network is unable to cope with it, that traffic (or portion of it) could be dropped.

1.2 Contribution of this Work

In [17], real time algorithms are proposed to predict the size of B-frames for MPEG-4 video traffic. Based on the results represented in that work and our own reservations about a simplification that was adopted by the authors in [17], we tried to confirm whether the same methodology also fits for H.264 videos. As it will be analyzed in the following chapter, we found that the approach used in [17] did not provide satisfactory results in the case of H.264 videos. Hence we kept the basic idea from [17] but used a different technique based on linear regression in order to achieve much higher modeling accuracy.

Our work focuses on the prediction of the size of the B-frames of the GOP for H.264 video. At first, we analyze the variability of the different frame types of the GOP. We compare their sizes to reach conclusions regarding their importance in the GOP's structure and then we focused on the autocorrelations of B-frames and cross correlation between B-frames and P- and I-frames. We implement three prediction models and after comparing their results, we conclude which models offer the highest accuracy.

CHAPTER 2: TRAFFIC CHARACTERISTICS OF H.264 ENCODED VIDEO

2.1 Bit rate variability

The first step in our work is to analyze the rate variability of the different frame types of the GOP's structure. Similarly to [17], we use the coefficient of variation (CoV) of the frame sizes to represent the rate variability. For a video sequence consisting of M frames encoded with a given quantization level, if X_m(m=1,2,…,M) denotes the sizes of the encoded video frames , then the CoV of the encoded video is defined in equation (1), where σ is the standard deviation and $\overline{X}$ is the mean of the frame sizes.

$$CoV = \frac{\sigma}{\overline{X}} = \frac{\sqrt{\frac{1}{(M-1)} \sum_{m=1}^{M}(X_m - \frac{1}{M}\sum_{m=1}^{M} X_m)^2}}{\frac{1}{M}\sum_{m=1}^{M} X_m} \quad (1)$$

We worked with 36 different H.264 video traces obtained from [2]. More specifically, we used the video traces of "Silence of the Lambs", "NBC-news" and "Star Wars IV" each one of them in 4 different types of GOP (G16B1, G16B3, G16B7 and G16B15) and each of them in low quality (QP=48), medium quality (QP=28) and high quality (QP=10). Firstly, we have computed the CoV of the frame sizes of the video traces including the B-frames. In order to observe how B-frames affect the rate variability of each movie, we then removed them from the whole video trace and used only the I- and P-frames to compute the new standard deviation and the mean. Finally we computed the CoV of the video traces without B-frames. The results are shown in Table 1.

It's easy to observe from the results that in all cases the coefficient of variation (CoV) is significantly reduced when B-frames are removed from the entire encoded video, i.e., the I and P frames have smaller variations in their sizes. Hence, the reduction of this rate variability leads to smoothing the encoded video bit stream. Another noteworthy observation is that in all cases, high quality video traces (QP=10) exhibit lower CoV than medium and low quality movies. This is expected as the more compressed a movie is the more likely it is to contain a few outliers leading to high CoV.

TABLE 1
COEFFICIENT OF VARIATION FOR THE WHOLE TRACE AND WHEN B-FRAMES ARE DROPPED

H264								
QP	**G16B1**		**G16B7**		**G16B15**		**G16B3**	
	Cov (With B-frames)	**Cov (Without B-frames)**	**Cov (With B-frames)**	**Cov (Without B-frames)**	**Cov (With B-frames)**	**Cov (Without B-frames)**	**Cov (With B-frames)**	**Cov (Without B-frames)**
Silence of the Lambs								
10	1.012	0.6781	1.0700	0.5517	0.9741	0.4871	1.1326	0.6138
28	2.334	1.6056	2.2713	1.0647	2.0676	0.8377	2.3435	1.3293
48	1.8336	1.4388	2.0788	0.9204	2.0912	0.7362	1.9884	1.8630
NBC-News								
10	0.33700	0.2360	0.3299	0.2394	0.3070	0.2254	0.3347	0.2425
28	1.3724	0.9537	1.4332	0.6224	1.2852	0.4172	1.4784	0.8063
48	1.8537	1.2862	2.1599	0.6939	2.1625	0.4018	2.0641	1,0058
Star Wars IV								
10	0.9946	0.6399	0.9918	0.4574	0.8650	0.3293	1.0543	0.5559
28	1.7452	1.2324	1.7610	0.7397	1.5735	0.4906	1.8341	0.9881
48	1.7088	1.3206	1,8111	0.7426	1.7188	0.4656	1.8139	1.0465

2.2 Size characteristics

For further analysis on how the B-frames dropping could affect the final movie playback we compare the size of B-frames with the size of I-frames, for all of the above movies. In Tables 2-4 we present the respective results.

TABLE 2
B-FRAME AND I-FRAME SIZE COMPARISON FOR SILENCE OF THE LAMBS

Qp	Total size of I-frames (bytes)	Total size of B-frames (bytes)	Mean size of I-frames (bytes)	Mean size of B-frames (bytes)	Mean size of the B-frames per GOP
Silence of the Lambs- G16B1					
10	76690052	73590131	22722.5	2725.7	21805
28	12713414	3409408	3766.9	126.28	1010.2
48	1258845	564928	372.99	20.924	167.38
Silence of the Lambs- G16B3					
10	77530556	182707761	22972,2	4511.62	54138.7
28	12840283	8833879	3804.5	218.1375	2617.62
48	1267193	943715	375,4625	23.30332	279.64
Silence of the Lambs- G16B7					
10	79915676	280520777	23678.72	5937.82	83127.5
28	13270213	15827428	3931.9	335.0154	4690.25
48	1292053	1295285	382.831	27.4175	383.83
Silence of the Lambs- G16B15					
10	82576054	370390711	24466.9	7318.5	109776.2
28	13892232	24626780	4116.21	486.599	7298.8
48	1329150	1693736	393.822	33.466	501.98

TABLE 3
B-FRAME AND I-FRAME SIZE COMPARISON FOR NBC NEWS

Qp	Total size of I-frames (bytes)	Total size of B-frames (bytes)	Mean size of I-frames (bytes)	Mean size of B-frames (bytes)	Mean size of the B-frames per GOP
NBC-News - G16B1					
10	140500106	553824726	45381.17	22366.25	178925
28	28351196	14828587	9157.36	598.868	4790.88
48	3158366	665200	1020.1	26.864	214.91
NBC-News - G16B3					
10	141533156	883877092	45714.84	23798.52	285575
28	82596732	31840452	9236.67	857.31	10287.5
48	3182014	1355213	1027.78	36.489	437.86
NBC-News - G16B7					
10	144403568	1091582316	46642	25192.3	352687.5
28	29368510	50668847	8485.9	1169.37	16371.2
48	3271438	2133861	1056.66	49.2457	689.437
NBC-News - G16B15					
10	147632775	1232330990	47685	26544.5	398162.5
28	30399183	7250628	9818.85	1561.8	23426.25
48	3439725	3117206	1111.02	67.145	1007,2

TABLE 4
B-FRAME AND I-FRAME SIZE COMPARISON FOR STAR WARS IV

Qp	Total size of I-frames (bytes)	Total size of B-frames (bytes)	Mean size of I-frames (bytes)	Mean size of B-frames (bytes)	Mean size of the B-frames per GOP
Star Wars IV - G16B1					
10	76808815	77408394	22758.17	2867.125	22936.25
28	13224204	4269580	3918.28	158.138	1265.15
48	1465665	626307	434.27	23.197	185.57
Star Wars IV - G16B3					
10	77503287	161119639	22963.9	3978.55	47741.25
28	13356362	10077450	3957.44	248.844	2986.125
48	1472281	1093690	436.23	27.006	324.07
Star Wars IV - G16B7					
10	79450408	243248760	23540.8	5148.88	72082.5
28	13779107	17560492	4082.69	371.706	5203.75
48	1498352	1602658	443.956	33.9237	474.925
Star Wars IV - G16B15					
10	81596064	329681301	24176.61	6514.15	97710
28	14356573	27168834	4253.79	536.83	8052.25
48	1545841	2209581	458.027	43.658	654.87

As expected, the mean size of I-frames in a trace is always larger than the mean size for B-frames. In a GOP though, we always have one I-frame and as many B-frames as the GOP structure indicates. We also observe the difference of the average size of I-frames with the mean size of B-frames per GOP. We should notice here that the results differ for every type of GOP because the number of B-frames per GOP changes. For example, by observing the results for the movie ‘Star Wars IV’-G16B1 we can see that the average size of B-frames per GOP is smaller than the average size of I-frames, with the exception of the high quality trace (QP=10) .This is so because in G16B1 there are only 8 B-frames per GOP. On the other hand in ‘Star Wars IV’- G16B15 the mean size of B-frames per GOP is always larger than the mean size of I-frames due to the fact that in a G16B15 GOP there are 15 B-frames and no P-frames. In addition, most of the times the total size of B-frames in a trace exceeds the total size of I-frames. In any case, a substantial portion of every GOP and every movie consists of B-frames, hence if we could successfully remove B-frames without causing image distortion we could achieve important bandwidth savings.

For this reason, despite the large differences in content, encoding quality and GOP structure among the 36 traces we studied, we tried to find a general B-frame traffic prediction model. Such a model can be used in order to reduce the bandwidth requirements and smoothen the encoded video stream by selective B-frames dropping, when the model predicts that the expected B-frame traffic will be larger than that which the network can handle.

CHAPTER 3: PREDICTING THE SIZE OF B-FRAMES

In order to achieve an accurate prediction for B-frames sizes, we have studied the way B-frames are correlated with the other types of frames. More specifically, as we have already mentioned B-frames are constructed based on the reference I and P frames; consequently, we expect that there might be a strong correlation with the size of those frames. Fig.1 illustrates the structure of the 4 GoP patterns that we have studied.

I	B1	P1	B2	P2	B3	P3	B4	P4	B5	P5	B6	P6	B7	P7	B8

(a)

I	B1	B2	B3	P1	B4	B5	B6	P2	B7	B8	B9	P3	B10	B11	B12

(b)

I	B1	B2	B3	B4	B5	B6	B7	P1	B8	B9	B10	B11	B12	B13	B14

(c)

I	B1	B2	B3	B4	B5	B6	B7	B8	B9	B10	B11	B12	B13	B14	B15

(d)

Fig.1. Encoded GOP sequence for (a) G16B1 (b) G16B3 (c) G16B7 (d) G16B15.

In a GOP, every B-frame has its own importance, so we must study separately each and every one's correlation with the other types of frames. In order to find the most relevant correlation in the short term, we compute the coefficient of correlation ($\rho_{X,Y}$) between each B-frame (variable X), and each I- or P- frame (variable Y) in a GOP using equation (2).

$$\rho_{X,Y} = \frac{E(XY) - \overline{XY}}{\sigma_X \, \sigma_Y} \quad (2)$$

where X and Y represent the size of the frames. σ_X and σ_Y represent the standard deviation of X and Y respectively. Some indicative correlation results are presented in Tables 5-7.

TABLE 5
CORRELATION COEFFICIENT OF DIFFERENT FRAMES OF STAR WARS IV G16B1 IN HQ

Star Wars IV- G16B1-QP=10								
	B1	**B2**	**B3**	**B4**	**B5**	**B6**	**B7**	**B8**
I	0,28659	0,291388	0,273166	0,278224	0,270814	0,270935	0,263906	0,257256
P1	**0,7416**	0,650853	0,625487	0,603945	0,565391	0,544645	0,599413	0,573457
P2	0,550125	**0,749193**	0,667739	0,652733	0,629431	0,543393	0,553268	0,612406
P3	0,600217	0,596216	**0,755475**	0,660447	0,637857	0,583746	0,571801	0,575614
P4	0,604249	0,629184	0,617305	**0,763073**	0,666143	0,621867	0,621766	0,587191
P5	0,574626	0,611617	0,610734	0,570581	**0,724055**	0,625186	0,618712	0,605727
P6	0,550953	0,586231	0,597642	0,599556	0,550734	**0,700522**	0,62871	0,600232
P7	0,555784	0,585771	0,596601	0,611452	0,59962	0,541415	**0,727179**	**0,637414**

TABLE 6
CORRELATION COEFFICIENT OF DIFFERENT FRAMES OF NBC NEWS G16B3 IN HQ

NBC-News- G16B3-QP=10												
	B1	**B2**	**B3**	**B4**	**B5**	**B6**	**B7**	**B8**	**B9**	**B10**	**B11**	**B12**
I	0,6573	0,6453	0,6519	0,6276	0,6152	0,6290	0,6055	0,5939	0,6135	0,5846	0,5671	0,5865
P1	**0,8294**	**0,8459**	**0,8647**	0,8252	0,8093	0,7900	0,7469	0,7468	0,7332	0,6996	0,6971	0,6856
P2	0,7554	0,7662	0,7790	**0,8516**	**0,8644**	**0,8737**	0,8163	0,8050	0,7836	0,7403	0,7346	0,7210
P3	0,7133	0,7244	0,7333	0,7714	0,7896	0,8024	**0,8561**	**0,8748**	**0,8890**	**0,8437**	**0,8207**	**0,7934**

TABLE 7
CORRELATION COEFFICIENT OF DIFFERENT FRAMES OF SILENCE OF THE LAMBS G16B1 IN HQ

Silence of the Lambs - G16B7-QP=10		
	I	**P1**
B1	0,572403	**0,735579**
B2	0,688087	**0,897167**
B3	0,68539	**0,907998**
B4	0,687395	**0,913087**
B5	0,692332	**0,9152**
B6	0,699424	**0,908864**
B7	0,580505	**0,749111**
B8	0,564558	**0,715227**
B9	0,682279	**0,884888**
B10	0,679062	**0,887973**
B11	0,674912	**0,887084**
B12	0,678313	**0,882795**
B13	0,678592	**0,872207**
B14	0,562311	**0,716618**

The values in bold show the strongest correlation for every B-frame. As we can see, for all cases the correlation between B-frames and I-frames is always weaker than the correlation between B- and P- frames. Even when B-frames are encoded with an I-frame as reference (for instance, the first B-frame in G16B1), the coefficient of correlation between them and the I-frame is lower than the coefficient of correlation between them and a P-frame (except of course in the case of G16B15 pattern, in which there are no P-frames).

Our next step was to compute the autocorrelation between the B-frames of a movie trace. In equation (3) X represents the size of the B-frame, σ_X represents the standard deviation of X and k is the lag. For instance, if we want to compute the autocorrelation for sequential B-frames we choose k=1.

$$r(k) = \frac{E[(X_m - \overline{X})(X_{m+k} - \overline{X})]}{\sigma_X^2} \qquad (3)$$

We have computed the autocorrelation for every movie using lags from 1 to 1000. Fig.2 presents some indicative results for different traces, qualities and GOP patterns.

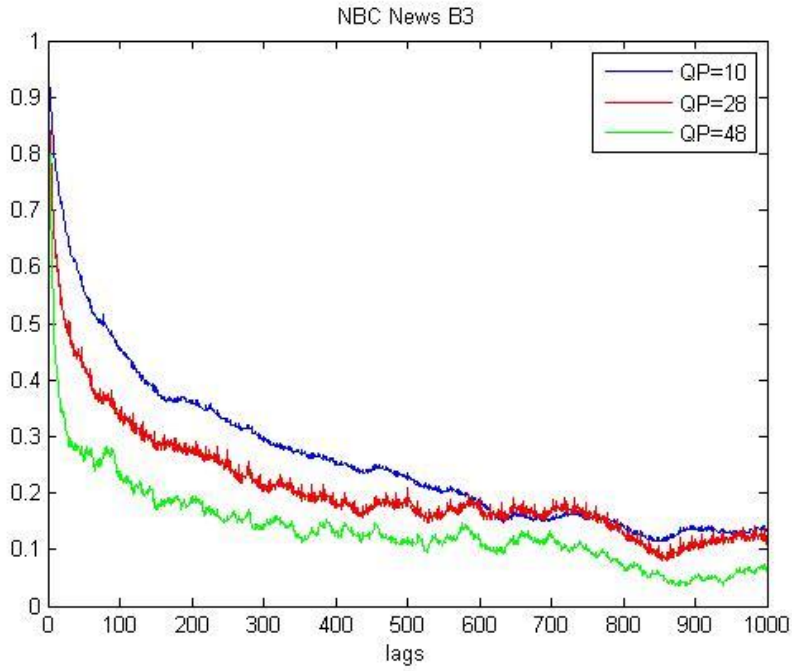

(a)

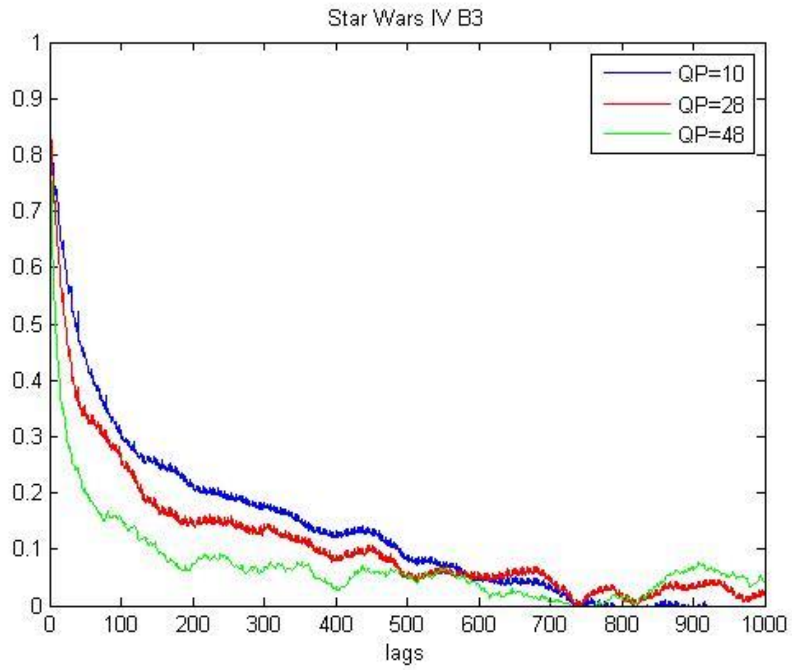

(b)

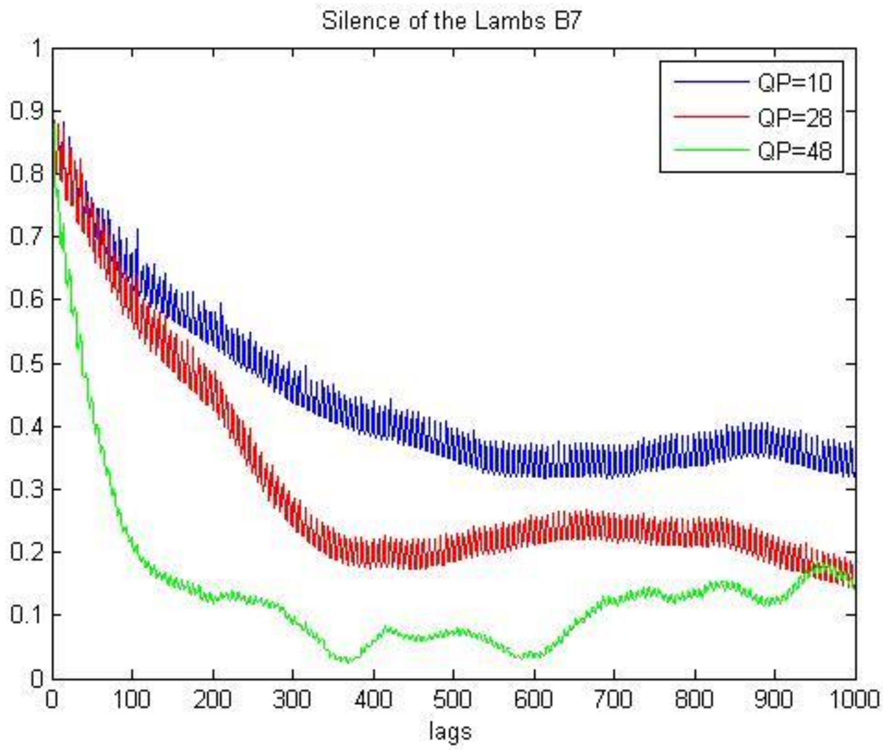

(c)

Fig.2. Autocorrelation of B-frames for (a) NBC news G16B3 (b) Star Wars IV G16B3 and (c) Silence of the Lambs G16B7 movies encoded in H.264 (LQ,MQ, and HQ)(1000 frame lags).

For the majority of the traces the values of the curves are very close to 1 for the first lags, indicating a strong Short Range Dependency (SRD), however the autocorrelation of B-frames quickly decreases, indicating an absence of Long Range Dependency (LRD). Also, comparing the autocorrelation of B-frames for the encoded videos in QP=10, QP=28, QP=48 we observe that the movies encoded in LQ (QP=48) exhibit lower B-frame autocorrelation. The autocorrelation values up to 1000 lags for all the trace under study can be found in the Appendix. These high levels of autocorrelation combined with our previous results on the coefficient of correlation between B- and P-frames can be used for an accurate prediction of the size of B-frames.

The values of the autocorrelation for lag=1 and for lag=2 are usually close to 1, but there are some cases (e.p. 'Silence of the lambs' G16B1) where the results are not so high for consecutive B-frames. As a consequence, we decided that the best way to achieve an accurate prediction by using inter frame correlation coefficient would be to use the two frames that have the highest correlation with the B-frame that we want to predict. Hence, we compared the values of autocorrelation for lag=1 and lag=2 with the highest values of coefficient of correlation for each B-frame. The two highest values were used for the prediction. More specifically, if the results of B-frame autocorrelation for lag=1 and lag=2 are higher than the correlation of the B-frame with any P-frames of the GOP, we use in our set of equations an equation for prediction that only includes the sizes of previous B-frames. On the other hand, if the correlation of the B-frame with any P-frame is stronger than the autocorrelation with any other B-frame, then we use that P-frame in our set of equations. In conclusion, for the prediction of each B frame's size in the next GOP we use exactly two previous frames (B or P), those that we found on average to have the highest correlation with the specific B frame over all GOPs of the trace.

To define the size of the first B-frame of the t^{th} GOP of each movie we used the notation $B_{1,t}$ and in the same way we continued for the rest of the B- and P-frames (B2, B3, B4, B5, P1…). All these vectors have the same length which represents the number of GOPs in the encoded video trace. Depending on the trace's GOP pattern, the length of vector B changes. For instance if the trace uses the G16B1 pattern, then B_t= [$B_{1,t}$,$B_{2,t}$, $B_{3,t}$, $B_{4,t}$, $B_{5,t}$, $B_{6,t}$, $B_{7,t}$, $B_{8,t}$], otherwise for G16B7 B_t= [$B_{1,t}$,$B_{2,t}$, $B_{3,t}$, $B_{4,t}$, $B_{5,t}$, $B_{6,t}$, $B_{7,t}$, $B_{8,t}$, $B_{9,t}$, $B_{10,t}$, $B_{11,t}$, $B_{12,t}$, $B_{13,t}$,$B_{14,t}$].

3.1 The model based on autocorrelation and cross correlation

We employ a linear regression-type model of prediction for each encoded movie according to the rules mentioned above. Two indicative examples are represented in (4) and (5), where the sets of equations for the prediction of the size of each B-frame contain the frames with the highest correlation with that frame. This approach differs with the one proposed in [17], which will be explained in Section 3.2.

NBC-G16B1-QP=10

$$
\begin{aligned}
\widehat{B}_{1,t} &= a_1 P_{1,t} + \gamma_1 B_{8,t-1} \\
\widehat{B}_{2,t} &= a_2 P_{2,t} + \gamma_2 B_{1,t} \\
\widehat{B}_{3,t} &= a_3 P_{3,t} + \gamma_3 B_{2,t} \\
\widehat{B}_{4,t} &= a_4 P_{4,t} + \gamma_4 B_{3,t} \\
\widehat{B}_{5,t} &= a_5 P_{5,t} + \gamma_5 B_{4,t} \\
\widehat{B}_{6,t} &= a_6 P_{6,t} + \gamma_6 B_{5,t} \\
\widehat{B}_{7,t} &= a_7 P_{7,t} + \gamma_7 B_{6,t} \\
\widehat{B}_{8,t} &= a_8 B_{7,t} + \gamma_8 B_{6,t}
\end{aligned} \quad (4)
$$

Star Wars IV-G16B3-QP=10

$$
\begin{aligned}
\widehat{B}_{1,t} &= a_1 B_{11,t-1} + \gamma_1 B_{12,t-1} \\
\widehat{B}_{2,t} &= a_2 B_{12,t-1} + \gamma_2 B_{1,t-1} \\
\widehat{B}_{3,t} &= a_3 B_{1,t} + \gamma_3 B_{2,t} \\
\widehat{B}_{4,t} &= a_4 B_{2,t} + \gamma_4 B_{3,t} \\
\widehat{B}_{5,t} &= a_5 B_{3,t} + \gamma_5 B_{4,t} \\
\widehat{B}_{6,t} &= a_6 B_{4,t} + \gamma_6 B_{5,t} \\
\widehat{B}_{7,t} &= a_7 B_{5,t} + \gamma_7 B_{6,t} \\
\widehat{B}_{8,t} &= a_8 B_{6,t} + \gamma_8 B_{7,t} \\
\widehat{B}_{9,t} &= a_9 B_{7,t} + \gamma_9 B_{8,t} \\
\widehat{B}_{10,t} &= a_{10} B_{8,t} + \gamma_{10} B_{9,t} \\
\widehat{B}_{11,t} &= a_{11} B_{9,t} + \gamma_{11} B_{10,t} \\
\widehat{B}_{12,t} &= a_{12} B_{10,t} + \gamma_{12} B_{11,t}
\end{aligned} \quad (5)
$$

We used the least squares method on Matlab to compute the coefficients α_j and γ_j with j ranging from 1 to the number of B-frames in a GOP (depending on the GOP pattern, this number can be equal to 8, 12, 14, or 15). We have computed 36 different tables of α_j and γ_j values for each encoded video that we worked with. The values of α_j and γ_j for the above two sets of equations are presented in Tables 8 and 9. The predicted values for all B-frames of all encoded videos are given by (4) and (5) when inserting the α_j and γ_j values.

TABLE 8

COEFFICIENTS' VALUES OBTAINED USING THE LEAST SQUARES METHOD AND (4) FOR NBC NEWS G16B1 WITH QP=10

NBC-G16B1-QP=10								
	B-1	**B-2**	**B-3**	**B-4**	**B-5**	**B-6**	**B-7**	**B-8**
α	0,334024	0,334024	0,334024	0,334024	0,334024	0,334024	0,334024	0,334024
γ	0,484232	0,484232	0,484232	0,484232	0,484232	0,484232	0,484232	0,484232

TABLE 9

COEFFICIENTS' VALUES OBTAINED USING THE LEAST SQUARES METHOD AND (5) FOR STAR WARS IV G16B3 WITH QP=10

Star-G16B3-QP=10		
	α	**γ**
B-1	0,990649	0,154828
B-2	0,966987	0,358207
B-3	0,105641	0,856314
B-4	0,966329	0,729002
B-5	0,960603	0,081054
B-6	0,227202	0,721576
B-7	0,974034	0,405562
B-8	1,039144	-0,12039
B-9	0,064857	0,837264
B-10	1,022473	0,013752
B-11	0,967071	-0,0274
B-12	0,276812	0,659793

To define the accuracy of our results and to compute the difference from the actual value of the B-frame, we used the Relative Percentage Error (RPE) defined in equation (6).

$$RPE = \frac{\sum_{m=1}^{L} \varepsilon_m}{\sum_{m=1}^{L} X_m} \times 100\% \quad (6)$$

L is the number of GOPs in the encoded video, X is the actual size of the frame and ε is the marginal error. In (7) we define the marginal error as the difference between the predicted size of the frame and its actual size [17]. $\hat{X}_m$ is the predicted size of the B-frame and X_m is the actual size.

$$\varepsilon_m = \hat{X}_m - X_m \quad (7)$$

The RPE results for the model we have described are shown in Tables 10-12. For the majority of the movies the RPE is low, which implies that the model is accurate. However, a very high RPE is observed for the movie 'Silence of the Lambs' G16B1 for QP=10 and QP=28 (high and medium quality). For these two encoded traces the sets of equations that we have computed are the only ones that use only P-frames because the B-frame autocorrelation for lag=1 and lag=2 was very low. By studying the results we notice that the prediction equations that use P-frames more than B-frames have higher RPE. As shown from the results, our approach gives relatively low RPE results for the majority of the encoded videos.

TABLE 10
RELATIVE PERCENTAGE ERROR FOR B-FRAME SIZE PREDICTION FOR STAR WARS IV

	RPE
Star Wars IV G16B1-Qp=10	-20.28%
Star Wars IV G16B1-Qp=28	16.43%
Star Wars IV G16B1-Qp=48	3.52%
Star Wars IV G16B3-Qp=10	13.25%
Star Wars IV G16B3-Qp=28	7.11%
Star Wars IV G16B3-Qp=48	1.74%
Star Wars IV G16B7-Qp=10	6.6%
Star Wars IV G16B7-Qp=28	5.45%
Star Wars IV G16B7-Qp=48	1.77%
Star Wars IV G16B15-Qp=10	6%
Star Wars IV G16B15-Qp=28	4.52%
Star Wars IV G16B15-Qp=48	1.39%

TABLE 11
RELATIVE PERCENTAGE ERROR FOR B-FRAME SIZE PREDICTION FOR SILENCE OF THE LAMBS.

	RPE
Silence of the Lambs G16B1-Qp=10	-99.86%
Silence of the Lambs G16B1-Qp=28	96.95%
Silence of the Lambs G16B1-Qp=48	2.52%
Silence of the Lambs G16B3-Qp=10	-14.09%
Silence of the Lambs G16B3-Qp=28	4.57%
Silence of the Lambs G16B3-Qp=48	1.4%
Silence of the Lambs G16B7-Qp=10	-34.9%
Silence of the Lambs G16B7-Qp=28	4.9%
Silence of the Lambs G16B7-Qp=48	1.24%
Silence of the Lambs G16B15-Qp=10	9.18%
Silence of the Lambs G16B15-Qp=28	-1.08%
Silence of the Lambs G16B15-Qp=48	1%

TABLE 12
RELATIVE PERCENTAGE ERROR FOR B-FRAME SIZE PREDICTION FOR NBC NEWS.

	RPE
NBC news G16B1-Qp=10	-0.19%
NBC news G16B1-Qp=28	32.1%
NBC news G16B1-Qp=48	4.42%
NBC news G16B3-Qp=10	0.28%
NBC news G16B3-Qp=28	14.99%
NBC news G16B3-Qp=48	3.54%
NBC news G16B7-Qp=10	0.24%
NBC news G16B7-Qp=28	9.58%
NBC news G16B7-Qp=48	3.32%
NBC news G16B15-Qp=10	0.2%
NBC news G16B15-Qp=28	7.34%
NBC news G16B15-Qp=48	2.54%

3.2 Model based on Silence of the Lambs Qp=10 trace

In order to find a model that accurately predicts the B frames' sizes for all movies, we decided to try a different technique on how the sets of equations for each trace will be formed. We tested if the prediction approach for the B-frames' sizes in [17] performs well for our H.264 movies. The idea in [17] is to derive a linear regression model for one trace (the Silence of the Lambs High Quality MPEG-4 trace) and implement it over all the traces under study, for simplicity reasons. Then, depending on the results, the authors "tweak" their model by changing a couple of equations for specific B frames if the results they derive are not satisfactory for a specific trace.

Similarly to the approach of [17], in this part of our work we chose 4 encoded video traces, which were also versions of the 'Silence of the lambs' trace (which was used in [17], as well) for QP=10 with G16B1, G16B3, G16B7 and G16B15. We followed the same procedure as in the previous Section for these 4 videos. We used the sets of equations in (8) and (9) and the results for the coefficients α_j and γ_j in Tables 13-16.

The next step was to apply these sets of equations on the rest of the movies, similarly to [17], depending on the GOP pattern they follow. More specifically, for all the encoded movies with G16B1 (for all types of qualities) we have employed the set of equations of the 'Silence of the Lambs' G16B1 QP=10. For the encoded videos with G16B3 we used the set of equations of the 'Silence of the Lambs' G16B3 QP=10. Likewise, 'Silence of the Lambs' G16B7 QP=10 equations were used for all G16B7 movies and finally we implemented the set of equations of the 'Silence of the Lambs' G16B15 QP=10 for all encoded videos with G16B15.

We employ the least squares method, on Matlab, to find the new coefficients α_j and γ_j for all video traces and we compute the sizes of the B-frames from the equations, as well as the marginal error from (7) in order to compute the RPE. The RPE values for all encoded traces are shown in Tables 17-19.

(8)

Silence of the lambs-G16B1-QP=10

$$\hat{B}_{1,t} = a_1 P_{1,t} + \gamma_1 P_{4,t}$$
$$\hat{B}_{2,t} = a_2 P_{2,t} + \gamma_2 P_{5,t}$$
$$\hat{B}_{3,t} = a_3 P_{3,t} + \gamma_3 P_{6,t}$$
$$\hat{B}_{4,t} = a_4 P_{4,t} + \gamma_4 P_{1,t}$$
$$\hat{B}_{5,t} = a_5 P_{5,t} + \gamma_5 P_{2,t}$$
$$\hat{B}_{6,t} = a_6 P_{6,t} + \gamma_6 P_{3,t}$$
$$\hat{B}_{7,t} = a_7 P_{7,t} + \gamma_7 P_{4,t}$$
$$\hat{B}_{8,t} = a_8 P_{5,t} + \gamma_8 P_{3,t}$$

Silence of the lambs-G16B3-QP=10

$$\hat{B}_{1,t} = a_1 P_{1,t} + \gamma_1 P_{2,t}$$
$$\hat{B}_{2,t} = a_2 P_{1t} + \gamma_2 P_{2,t}$$
$$\hat{B}_{3,t} = a_3 P_{1,t} + \gamma_3 P_{2,t}$$
$$\hat{B}_{4,t} = a_4 P_{2,t} + \gamma_4 P_{3,t}$$
$$\hat{B}_{5,t} = a_5 P_{2,t} + \gamma_5 P_{1,t}$$
$$\hat{B}_{6,t} = a_6 P_{2,t} + \gamma_6 P_{1,t}$$
$$\hat{B}_{7,t} = a_7 P_{3,t} + \gamma_7 P_{1,t}$$
$$\hat{B}_{8,t} = a_8 P_{3,t} + \gamma_8 P_{2,t}$$
$$\hat{B}_{9,t} = a_9 P_{3,t} + \gamma_9 P_{2,t}$$
$$\hat{B}_{10,t} = a_{10} P_{2,t} + \gamma_{10} P_{1,t}$$
$$\hat{B}_{11,t} = a_{11} P_{3,t} + \gamma_{11} P_{2,t}$$
$$\hat{B}_{12,t} = a_{12} P_{3,t} + \gamma_{12} P_{1,t}$$

TABLE 13
VALUES OF COEFFICIENT FOR SILENCE OF THE LAMBS G16B1 WITH QP=10

Silence-G16B1-QP=10		
	α	**γ**
B-1	0,207393	-0,01339
B-2	0,030884	0,164316
B-3	0,15095	0,036438
B-4	0,062841	0,136246
B-5	0,064009	0,133795
B-6	0,115947	0,072768
B-7	0,049843	0,144585
B-8	0,441481	-0,24179

TABLE 14
VALUES OF COEFFICIENT FOR SILENCE OF THE LAMBS G16B3 WITH QP=10

Silence-G16B3-QP=10		
	α	**γ**
B-1	0,191536	0,058326
B-2	0,205266	0,110768
B-3	0,213629	0,044942
B-4	0,156577	0,095701
B-5	0,04798	0,280695
B-6	0,069486	0,193862
B-7	0,144673	0,105046
B-8	0,121556	0,199197
B-9	0,126901	0,12751
B-10	1,045723	-0,84319
B-11	0,10425	0,223243
B-12	0,49673	-0,19673

(9)

Silence of the lambs-G16B7-QP=10

$$\hat{B}_{1,t} = a_1 B_{13,t-1} + \gamma_1 B_{14,t-1}$$
$$\hat{B}_{2,t} = a_2 P_{1,t} + \gamma_2 B_{1,t}$$
$$\hat{B}_{3,t} = a_3 P_{1,t} + \gamma_3 B_{2,t}$$
$$\hat{B}_{4,t} = a_4 P_{1,t} + \gamma_4 B_{3,t}$$
$$\hat{B}_{5,t} = a_5 P_{1,t} + \gamma_5 B_{4,t}$$
$$\hat{B}_{6,t} = a_6 P_{1,t} + \gamma_6 B_{5,t}$$
$$\hat{B}_{7,t} = a_7 B_{5,t} + \gamma_7 B_{6,t}$$
$$\hat{B}_{8,t} = a_8 B_{6,t} + \gamma_8 B_{7,t}$$
$$\hat{B}_{9,t} = a_9 B_{8,t} + \gamma_9 P_{1,t}$$
$$\hat{B}_{10,t} = a_{10} P_{1,t} + \gamma_{10} B_{9,t}$$
$$\hat{B}_{11,t} = a_{11} P_{1,t} + \gamma_{11} B_{10,t}$$
$$\hat{B}_{12,t} = a_{12} B_{11,t} + \gamma_{12} P_{1,t}$$
$$\hat{B}_{13,t} = a_{13} B_{12,t} + \gamma_{13} P_{1,t}$$
$$\hat{B}_{14,t} = a_{14} B_{12,t} + \gamma_{14} B_{13,t}$$

Silence of the lambs-G16B15-QP=10

$$\hat{B}_{1,t} = a_1 B_{11,t-1} + \gamma_1 B_{12,t-1}$$
$$\hat{B}_{2,t} = a_2 B_{12,t-1} + \gamma_2 B_{1,t}$$
$$\hat{B}_{3,t} = a_3 B_{1,t} + \gamma_3 B_{2,t}$$
$$\hat{B}_{4,t} = a_4 B_{2,t} + \gamma_4 B_{3,t}$$
$$\hat{B}_{5,t} = a_5 B_{3,t} + \gamma_5 B_{4,t}$$
$$\hat{B}_{6,t} = a_6 B_{4,t} + \gamma_6 B_{5,t}$$
$$\hat{B}_{7,t} = a_7 B_{5,t} + \gamma_7 B_{6,t}$$
$$\hat{B}_{8,t} = a_8 B_{6,t} + \gamma_8 B_{7,t}$$
$$\hat{B}_{9,t} = a_9 B_{7,t} + \gamma_9 B_{8,t}$$
$$\hat{B}_{10,t} = a_{10} B_{8,t} + \gamma_{10} B_{9,t}$$
$$\hat{B}_{11,t} = a_{11} B_{9,t} + \gamma_{11} B_{10,t}$$
$$\hat{B}_{12,t} = a_{12} B_{10,t} + \gamma_{12} B_{11,t}$$
$$\hat{B}_{13,t} = a_{13} B_{11,t} + \gamma_{13} B_{12,t}$$
$$\hat{B}_{14,t} = a_{14} B_{12,t} + \gamma_{14} B_{13,t}$$
$$\hat{B}_{15,t} = a_{15} B_{13,t} + \gamma_{15} B_{14,t}$$

TABLE 15
VALUES OF COEFFICIENT FOR SILENCE OF THE LAMBS G16B7 WITH QP=10

Silence-G16B7-QP=10		
	α	γ
B-1	0,994131	0,719739
B-2	0,397142	-8,42423
B-3	0,029092	1,023853
B-4	0,011949	1,006573
B-5	0,030757	0,900129
B-6	0,004304	0,909247
B-7	-0,01059	0,717334
B-8	0,99139	0,3722
B-9	0,665345	0,173029
B-10	0,013642	1,050924
B-11	0,003353	1,016096
B-12	1,002367	-0,00698
B-13	1,232202	-0,1106
B-14	-0,00825	0,698857

TABLE 16
VALUES OF COEFFICIENT FOR SILENCE OF THE LAMBS G16B15 WITH QP=10

Silence-G16B15-QP=10		
	α	γ
B-1	0,989609	0,778145
B-2	0,982551	1,253596
B-3	-0,126	1,325664
B-4	-0,07228	1,174036
B-5	-0,0812	1,154814
B-6	-0,03356	1,074077
B-7	-0,00252	1,02978
B-8	-0,03714	1,049402
B-9	0,067686	0,939517
B-10	-0,02795	1,018523
B-11	-0,00252	0,974149
B-12	-0,00432	0,955293
B-13	0,082157	0,833798
B-14	-0,01761	0,881737
B-15	-0,00508	0,669496

TABLE 17
RELATIVE PERCENTAGE ERROR FOR B-FRAME SIZE PREDICTION FOR SILENCE OF THE LAMBS

	RPE(based on Silence of the Lambs QP=10)
Silence of the Lambs G16B1-Qp=10	-99.86%
Silence of the Lambs G16B1-Qp=28	-97.75%
Silence of the Lambs G16B1-Qp=48	-53.5%
Silence of the Lambs G16B3-Qp=10	-14.09%
Silence of the Lambs G16B3-Qp=28	-10.51%
Silence of the Lambs G16B3-Qp=48	99.33%
Silence of the Lambs G16B7-Qp=10	-34.9%
Silence of the Lambs G16B7-Qp=28	-0.95%
Silence of the Lambs G16B7-Qp=48	1.49%
Silence of the Lambs G16B15-Qp=10	9.18%
Silence of the Lambs G16B15-Qp=28	-1.08%
Silence of the Lambs G16B15-Qp=48	1%

TABLE 18
RELATIVE PERCENTAGE ERROR FOR B-FRAME SIZE PREDICTION FOR NBC NEWS

	RPE(based on Silence of the Lambs QP=10)
NBC news G16B1-Qp=10	-6.79%
NBC news G16B1-Qp=28	-96.68%
NBC news G16B1-Qp=48	-80.01%
NBC news G16B3-Qp=10	-0.1%
NBC news G16B3-Qp=28	-15.24%
NBC news G16B3-Qp=48	81.76%
NBC news G16B7-Qp=10	0.16%
NBC news G16B7-Qp=28	5.26%
NBC news G16B7-Qp=48	2.55%
NBC news G16B15-Qp=10	0.2%
NBC news G16B15-Qp=28	7.34%
NBC news G16B15-Qp=48	2.54%

TABLE 19
RELATIVE PERCENTAGE ERROR FOR B-FRAME SIZE PREDICTION FOR STAR WARS IV

	RPE(βάση του Silence of the Lambs QP=10)
Star Wars IV G16B1-Qp=10	-99.82%
Star Wars IV G16B1-Qp=28	-97.79%
Star Wars IV G16B1-Qp=48	-59.41%
Star Wars IV G16B3-Qp=10	-9.44%
Star Wars IV G16B3-Qp=28	-0.34%
Star Wars IV G16B3-Qp=48	81.76%
Star Wars IV G16B7-Qp=10	-1.32%
Star Wars IV G16B7-Qp=28	0.87%
Star Wars IV G16B7-Qp=48	2.09%
Star Wars IV G16B15-Qp=10	6%
Star Wars IV G16B15-Qp=28	4.52%
Star Wars IV G16B15-Qp=48	1.39%

The results when using this modeling approach are clearly worse. The values of RPE for the encoded videos with G16B15 didn't change due to the fact that in both techniques the set of equations that have been used are the same. That happened because in all cases of the particular GOP pattern, there are no P-frames in the GOP, hence we can only use the information that the previous B-frames can give.

Especially for the LQ movies a huge increase in RPE can be observed for the majority of them. Unlike the first model that gives very low values of the RPE for most traces, the second model underperforms in terms of accuracy. This is expected, given the vastly different trace characteristics and their different compression. Also, as noted in [17], where the RPE for LQ movies was also higher, the autocorrelation for B-frames is typically lower in LQ movies than in HQ or MQ, therefore this result is again expected. Still, the results for some of the encoded videos, like G16B15 traces where only the information of the previous B-frames is used for prediction or G16B7 traces where more B- than P- frames are used, reveal very low values for the

RPE. That led us to test a new modeling approach where we use only the information of immediately previous B-frames for prediction. This approach is discussed in the next section.

3.3 Model based only on previous B-frames.

In Section 3.1 we used 36 different sets of equations for each of the 36 encoded video traces. We have utilized the information of the autocorrelation between the B-frames and the coefficient of correlation between B- and P- frames, to decide how we will build the equations. However, a large portion of these sets seems to use only B-frames; the reason is the high levels of autocorrelation among the B-frames in those traces. As already discussed in the previous sections, the values of RPE were low for these cases. Hence, we decided to create a model that predict the size of the next B-frame taking into account only the previous 2 B-frames of the trace. This approach was evaluated in [17], but was shown to perform worse than the authors' approach, which we implemented in Section 3.2.

The single set of equations that we will use for all of the 36 video traces is presented in Equation (10). Of course for every different GOP pattern the number of equations varies between 8, 12, 14, and 15 but, still follows the same notion.

G16B1

$$\hat{B}_{1,t} = a_1 B_{7,t-1} + \gamma_1 B_{8,t-1}$$
$$\hat{B}_{2,t} = a_2 B_{8,t-1} + \gamma_2 B_{1,t}$$
$$\hat{B}_{3,t} = a_3 B_{1,t} + \gamma_3 B_{2,t}$$
$$\hat{B}_{4,t} = a_4 B_{2,t} + \gamma_4 B_{3,t}$$
$$\hat{B}_{5,t} = a_5 B_{3,t} + \gamma_5 B_{4,t}$$
$$\hat{B}_{6,t} = a_6 B_{4,t} + \gamma_6 B_{5,t}$$
$$\hat{B}_{7,t} = a_7 B_{5,t} + \gamma_7 B_{6,t}$$
$$\hat{B}_{8,t} = a_8 B_{6,t} + \gamma_8 B_{7,t}$$

G16B7

$$\hat{B}_{1,t} = a_1 B_{13,t-1} + \gamma_1 B_{14,t-1}$$
$$\hat{B}_{2,t} = a_2 B_{14,t-1} + \gamma_2 B_{1,t}$$
$$\hat{B}_{3,t} = a_3 B_{1,t} + \gamma_3 B_{2,t}$$
$$\hat{B}_{4,t} = a_4 B_{2,t} + \gamma_4 B_{3,t}$$
$$\hat{B}_{5,t} = a_5 B_{3,t} + \gamma_5 B_{4,t}$$
$$\hat{B}_{6,t} = a_6 B_{4,t} + \gamma_6 B_{5,t}$$
$$\hat{B}_{7,t} = a_7 B_{5,t} + \gamma_7 B_{6,t}$$
$$\hat{B}_{8,t} = a_8 B_{6,t} + \gamma_8 B_{7,t}$$
$$\hat{B}_{9,t} = a_9 B_{7,t} + \gamma_9 B_{8,t}$$
$$\hat{B}_{10,t} = a_{10} B_{8,t} + \gamma_{10} B_{9,t}$$
$$\hat{B}_{11,t} = a_{11} B_{9,t} + \gamma_{11 B_{10,t}}$$
$$\hat{B}_{12,t} = a_{12} B_{10,t} + \gamma_{12 B_{11,t}}$$
$$\hat{B}_{13,t} = a_{13} B_{11,t} + \gamma_{13 B_{12,t}}$$
$$\hat{B}_{14,t} = a_{14} B_{12,t} + \gamma_{14} B_{13,t}$$

(10)

After using the least squares method again in order to find the coefficients α_j and γ_j we compute the marginal error and the Relative Percentage error (RPE) from (7) and (6). The results are shown in Tables 20-22.

TABLE 20
RELATIVE PERCENTAGE ERROR FOR B-FRAME SIZE PREDICTION FOR SILENCE OF THE LAMBS

	RPE (Based only on previous B-frames)
Silence of the Lambs G16B1-Qp=10	904%
Silence of the Lambs G16B1-Qp=28	16.86%
Silence of the Lambs G16B1-Qp=48	16.5%
Silence of the Lambs G16B3-Qp=10	57.69%
Silence of the Lambs G16B3-Qp=28	9.21%
Silence of the Lambs G16B3-Qp=48	1.4%
Silence of the Lambs G16B7-Qp=10	17.34
Silence of the Lambs G16B7-Qp=28	4.9%
Silence of the Lambs G16B7-Qp=48	1.24%
Silence of the Lambs G16B15-Qp=10	9.18%
Silence of the Lambs G16B15-Qp=28	-1.08%
Silence of the Lambs G16B15-Qp=48	1%

TABLE 21
RELATIVE PERCENTAGE ERROR FOR B-FRAME SIZE PREDICTION FOR NBC NEW

	RPE (Based only on previous B-frames)
NBC news G16B1-Qp=10	0.4%
NBC news G16B1-Qp=28	32.1%
NBC news G16B1-Qp=48	5.6%
NBC news G16B3-Qp=10	0.28%
NBC news G16B3-Qp=28	14.99%
NBC news G16B3-Qp=48	3.54%
NBC news G16B7-Qp=10	0.24%
NBC news G16B7-Qp=28	9.58%
NBC news G16B7-Qp=48	3.32%
NBC news G16B15-Qp=10	0.2%
NBC news G16B15-Qp=28	7.34%
NBC news G16B15-Qp=48	2.54%

TABLE 22
RELATIVE PERCENTAGE ERROR FOR B-FRAME SIZE PREDICTION FOR STAR WARS IV

	RPE (Based only on previous B-frames)
Star Wars IV G16B1-Qp=10	57.77%
Star Wars IV G16B1-Qp=28	13.76%
Star Wars IV G16B1-Qp=48	3.08%
Star Wars IV G16B3-Qp=10	13.25%
Star Wars IV G16B3-Qp=28	7.11%
Star Wars IV G16B3-Qp=48	2.25%
Star Wars IV G16B7-Qp=10	6.6%
Star Wars IV G16B7-Qp=28	5.45%
Star Wars IV G16B7-Qp=48	1.77%
Star Wars IV G16B15-Qp=10	6%
Star Wars IV G16B15-Qp=28	4.52%
Star Wars IV G16B15-Qp=48	1.39%

With the exception of the 'Silence of the Lambs' G16B1 QP=10 trace, the RPE results of this modeling approach are much lower compared with the results of the second model and very close with the ones in our first model. Especially for LQ video traces, the RPE is steadily very low. This indicates that, contrary to the respective result in [17], using only the previous two B-frames for prediction can lead to quite accurate results for H.264 traces.

CHAPTER 4: COMPARING THE MODELS

In this chapter we compare the obtained results of the 3 modeling approaches per trace, in terms of the average absolute value of the RPE over all the traces. The mean RPE is computed over 35 of the 36 traces, i.e., we do not include in our computation the RPE results for the trace Silence of the Lambs G16B1 QP=10, in all of three cases, for which all modeling approaches fail, as shown in Table 23, which contains all of the RPE results.

TABLE 23
RELATIVE PERCENTAGE ERROR FOR B-FRAME SIZE PREDICTION FOR ALL MOVIES AND FOR THE 3 MODELS

	RPE(based on ac)	**RPE(based on Silence of the Lambs QP=10)**	**RPE (based only on previous B-frames)**
Silence of the Lambs G16B1-Qp=10	-99.86%	-99.86%	904%
Silence of the Lambs G16B1-Qp=28	96.95%	-97.75%	16.86%
Silence of the Lambs G16B1-Qp=48	2.52%	-53.5%	16.5%
Silence of the Lambs G16B3-Qp=10	-14.09%	-14.09%	57.69%
Silence of the Lambs G16B3-Qp=28	4.57%	-10.51%	9.21%
Silence of the Lambs G16B3-Qp=48	1.4%	99.33%	1.4%
Silence of the Lambs G16B7-Qp=10	-34.9%	-34.9%	17.34
Silence of the Lambs G16B7-Qp=28	4.9%	-0.95%	4.9%
Silence of the Lambs G16B7-Qp=48	1.24%	1.49%	1.24%
Silence of the Lambs G16B15-Qp=10	9.18%	9.18%	9.18%
Silence of the Lambs G16B15-Qp=28	-1.08%	-1.08%	-1.08%
Silence of the Lambs G16B15-Qp=48	1%	1%	1%

Mean RPE (Absolute Value) for the Silence of the Lambs	**15,6%**	**29.43%**	**12.4%**
NBC news G16B1-Qp=10	-0.19%	-6.79%	0.4%
NBC news G16B1-Qp=28	32.1%	-96.68%	32.1%
NBC news G16B1-Qp=48	4.42%	-80.01%	5.6%
NBC news G16B3-Qp=10	0.28%	-0.1%	0.28%
NBC news G16B3-Qp=28	14.99%	-15.24%	14.99%
NBC news G16B3-Qp=48	3.54%	81.76%	3.54%
NBC news G16B7-Qp=10	0.24%	0.16%	0.24%
NBC news G16B7-Qp=28	9.58%	5.26%	9.58%
NBC news G16B7-Qp=48	3.32%	2.55%	3.32%
NBC news G16B15-Qp=10	0.2%	0.2%	0.2%
NBC news G16B15-Qp=28	7.34%	7.34%	7.34%
NBC news G16B15-Qp=48	2.54%	2.54%	2.54%
Mean RPE (Absolute value) for the NBC news trace	**6.56%**	**24.88%**	**6.67%**
Star Wars IV G16B1-Qp=10	-20.28%	-99.82%	57.77%
Star Wars IV G16B1-Qp=28	16.43%	-97.79%	13.76%
Star Wars IV G16B1-Qp=48	3.52%	-59.41%	3.08%
Star Wars IV G16B3-Qp=10	13.25%	-9.44%	13.25%
Star Wars IV G16B3-Qp=28	7.11%	-0.34%	7.11%

Star Wars IV G16B3-Qp=48	1.74%	81.76%	2.25%
Star Wars IV G16B7-Qp=10	6.6%	-1.32%	6.6%
Star Wars IV G16B7-Qp=28	5.45%	0.87%	5.45%
Star Wars IV G16B7-Qp=48	1.77%	2.09%	1.77%
Star Wars IV G16B15-Qp=10	6%	6%	6%
Star Wars IV G16B15-Qp=28	4.52%	4.52%	4.52%
Star Wars IV G16B15-Qp=48	1.39%	1.39%	1.39%
Mean RPE (Absolute Value) for Star wars IV	**7.338%**	**30.3%**	**10.24%**
Mean RPE (Absolute Value)	**9.8326%**	**28.20%**	**9.77%**

As shown from the above results, the average RPE value for the second modeling approach is clearly the highest. The results of the other two methods are very close, with the average value of the RPE in the third technique being slightly lower overall, while the first technique (our proposal) excels over the majority of the 36 traces. Our proposal also excels in terms of the mean RPE for two of the three movies under study.

Still, the complexity of our modeling approach is much greater, as we had to design and apply 36 different sets of equations, one for each video trace. In terms of on-the-fly prediction, the third model is much simpler; for our approach to work equally well or better (since it provides better results for the majority of the traces) an online machine learning algorithm would have to be implemented, which would compute the inter-frame correlation coefficients as B frames arrive, in order to decide, accordingly, on the proper set of equations for the linear regression-based prediction.

5. Conclusions and Future Work

In this thesis we have implemented and tested 3 different modeling techniques for predicting the size of the B-frames of H.264 encoded videos. It has been demonstrated that two of the models provide accurate prediction for a variety of video traces with different GOP patterns and different qualities. These models use the autocorrelation between the B-frames and the cross correlation of B- and P-frames in a trace. The first of the two demands a different set of equations for each trace, hence increasing complexity, while the third, which uses only the previous two B-frames for prediction of the future B frames' sizes, has much lower complexity and comparable accuracy results. This third modeling approach was shown in the literature to underperform when used for MPEG-4 video traffic, therefore in future work we intend to implement both of the competent models on a wider variety of traces encoded with MPEG-4, H.264 and H.265 traffic in order to hopefully reach a more general conclusion on which model provides the highest accuracy. We also intend to work on exploiting Long Range Dependence among video frames in order to provide longer term prediction for the bandwidth that video traces will demand, and on proposing a machine learning algorithm which will make our proposal feasible for on-the-fly prediction.

REFERENCES

[1] D.Marpe, T.Wiegand, G.Sullivan, “The H.264/MPEG4 advanced video coding standard and its applications”, IEEE Communications Magazine Vol. 44, No. 8, 2006, pp. 134-143.

[2] “Trace Files and Statistics”. [Online]: http://trace.eas.asu.edu/h264/index.html

[3] A. Lazaris, P. Koutsakis and M. Paterakis, “A New Model for Video Traffic Originating from Multiplexed MPEG-4 Videoconference Streams”, Performance Evaluation Journal, Elsevier Publ., Vol. 65, No. 1, 2008, pp. 51-70.

[4] D.M. Lucantoni, M.F. Neuts, A.R. Reibman, Methods for performance evaluation of VBR video traffic models, IEEE/ACM Transactions on Networking Vol. 2, No. 2, 1994, pp. 176–180.

[5] M. Nomura, T. Fuji, N. Ohta, Basic characteristics of variable rate video coding in ATM environment, IEEE Journal on Selected Areas in Communications Vol. 7, No. 5, 1989, pp. 752–760.

[6] D.P. Heyman, A. Tabatabai, T.V. Lakshman, Statistical analysis and simulation study of video teleconference traffic in ATM networks, IEEE Transactions on Circuits and Systems for Video Technology Vol. 2, No. 1, 1992, pp. 49–59.

[7] A.M. Dawood, M. Ghanbari, Content-based MPEG video traffic modeling, IEEE Transactions on Multimedia Vol. 1, No. 1, 1999, pp. 77–87.

[8] K. Chandra, A.R. Reibman, Modeling one- and two-layer variable bit rate video, IEEE/ACM Transactions on Networking Vol. 7, No. 3, 1999, pp. 398–413.

[9] Q. Ren, H. Kobayashi, Diffusion approximation modeling for Markov modulated bursty traffic and its applications to bandwidth allocation in ATM networks, IEEE Journal on Selected Areas in Communications Vol. 16, No.5, 1998, pp. 679–691.

[10] D.P. Heyman, The GBAR source model for VBR videoconferences, IEEE/ACM Transactions on Networking Vol. 5, No. 4, 1997, pp. 554–560.

[11] M. Frey, S. Ngyuyen-Quang, A gamma-based framework for modeling variable-rate video sources: The GOP GBAR model, IEEE/ACM

Transactions on Networking Vol. 8, No. 6, 2000, pp. 710–719.

[12] H.S. Chin, J.W. Goodge, R. Griffiths, D.J. Parish, Statistics of video signals for viewphone-type pictures, IEEE Journal on Selected Areas in Communications Vol. 7, No. 5, 1989, pp. 826–832.

[13] R. Kishimoto, Y. Ogata, F. Inumaru, Generation interval distribution characteristics of packetized variable rate video coding data streams in an ATM network, IEEE Journal on Selected Areas in Communications Communications Vol. 7, No. 5, 1989, pp. 833–841.

[14] D.P. Heyman, T.V. Lakshman, A. Tabatabai, H. Heeke, Modeling teleconference traffic from VBR video coders, in: Proceedings of the IEEE

International Conference on Communications (ICC) 1994, New Orleans, USA, pp. 1744–1748.

[15] S. Xu, Z. Huang, A Gamma autoregressive video model on ATM networks, IEEE Transactions on Circuits and Systems Video Technology Vol. 8, No. 2, 1998, pp. 138–142.

[16] U.K. Sarkar, S. Ramakrishnan, D. Sarkar, Modeling full-length video using Markov-modulated gamma-based framework, IEEE/ACM

Transactions on Networking Vol.1, No. 4, 2003, pp. 638–649

[17]L. I. Lanfranchi, B. K. Bing, “MPEG-4 Bandwidth Prediction for Broadband Cable Networks, in IEEE Transactions in Broadcasting, Vol. 54, No.4, December 2008

APPENDIX A

In this Appendix we present indicatively some of our results for the coefficient of correlation based on equation (2) and the results of the autocorrelation only for B-frames based on equation (3).

Silence of the Lambs- G16B1-QP=10								
	B1	**B2**	**B3**	**B4**	**B5**	**B6**	**B7**	**B8**
I	0,460644	0,462257	0,456479	0,469168	0,464442	0,4366	0,470352	0,443558
P1	0,709223	0,598082	0,571044	0,648295	0,571874	0,599106	0,58616	0,595696
P2	0,578378	0,71726	0,561763	0,603337	0,625896	0,559878	0,627414	0,568422
P3	0,584387	0,588476	0,690261	0,58097	0,588966	0,606686	0,584917	0,610769
P4	0,635579	0,608375	0,569261	0,710117	0,584715	0,581598	0,633776	0,585564
P5	0,558997	0,641113	0,573553	0,566765	0,704076	0,559269	0,59241	0,629537
P6	0,613327	0,607597	0,627207	0,588499	0,587707	0,692178	0,583147	0,600438
P7	0,549371	0,614728	0,573139	0,602987	0,579081	0,548996	0,694768	0,574813

Silence of the Lambs- G16B1-QP=28								
	B1	**B2**	**B3**	**B4**	**B5**	**B6**	**B7**	**B8**
I	0,226127	0,233365	0,215293	0,233981	0,236344	0,217342	0,24218	0,223755
P1	0,734898	0,647886	0,594925	0,666743	0,617627	0,613676	0,642244	0,589519
P2	0,602921	0,747015	0,590101	0,632449	0,670048	0,544198	0,69167	0,577732
P3	0,624097	0,627727	0,698494	0,601513	0,674869	0,592133	0,625167	0,642197
P4	0,634697	0,645888	0,582142	0,708303	0,647838	0,594938	0,653928	0,576883
P5	0,554567	0,651023	0,605251	0,566166	0,738015	0,568089	0,636037	0,638377
P6	0,638472	0,6179	0,625074	0,596657	0,644747	0,697529	0,607277	0,631224
P7	0,535091	0,649164	0,590512	0,581086	0,640959	0,528348	0,681045	0,588236

Silence of the Lambs- G16B1-QP=48								
	B1	**B2**	**B3**	**B4**	**B5**	**B6**	**B7**	**B8**
I	0,063992	0,058029	0,060137	0,071684	0,083118	0,08257	0,092509	0,051168
P1	0,605094	0,476789	0,452483	0,463324	0,430317	0,419115	0,442817	0,38198
P2	0,448842	0,620036	0,471329	0,483122	0,461452	0,400047	0,472725	0,393338
P3	0,420105	0,45578	0,623267	0,458996	0,439442	0,411909	0,436315	0,387461
P4	0,444622	0,469496	0,488199	0,588816	0,491117	0,453101	0,497668	0,409449
P5	0,382709	0,442234	0,433744	0,441548	0,616912	0,450059	0,479437	0,415258
P6	0,412181	0,445016	0,445297	0,457049	0,490316	0,581995	0,510092	0,418994
P7	0,390237	0,454985	0,434505	0,444194	0,450629	0,441752	0,633436	0,432553

Star Wars IV- G16B3-QP=10												
	B1	**B2**	**B3**	**B4**	**B5**	**B6**	**B7**	**B8**	**B9**	**B10**	**B11**	**B12**
I	0,34191	0,365545	0,335424	0,322519	0,355678	0,324752	0,313865	0,353838	0,31105	0,304878	0,332993	0,315858
P1	0,679373	0,777654	0,741204	0,696341	0,749469	0,680119	0,644759	0,70636	0,576049	0,575268	0,666695	0,622476
P2	0,638186	0,720465	0,650447	0,723298	0,798888	0,745212	0,688133	0,756601	0,650216	0,639604	0,692507	0,612303
P3	0,582185	0,651974	0,611771	0,61932	0,682555	0,606652	0,668068	0,766412	0,69602	0,650576	0,708389	0,634427

Star Wars IV- G16B3-QP=28												
	B1	**B2**	**B3**	**B4**	**B5**	**B6**	**B7**	**B8**	**B9**	**B10**	**B11**	**B12**
I	0,228744	0,239687	0,226251	0,213869	0,223861	0,208152	0,204773	0,227346	0,198882	0,203404	0,211871	0,207272
P1	0,663977	0,73227	0,703325	0,677421	0,712691	0,665471	0,625369	0,672378	0,587458	0,560627	0,620962	0,590455
P2	0,629795	0,692119	0,656672	0,724095	0,768749	0,723473	0,670103	0,719227	0,642866	0,61356	0,651551	0,611764
P3	0,548142	0,607965	0,579421	0,608583	0,654682	0,615596	0,671378	0,714813	0,658107	0,628156	0,660486	0,619483

Star Wars IV- G16B3-QP=48												
	B1	**B2**	**B3**	**B4**	**B5**	**B6**	**B7**	**B8**	**B9**	**B10**	**B11**	**B12**
I	0,152918	0,143157	0,159311	0,144701	0,131325	0,129597	0,153992	0,130391	0,132692	0,151709	0,110761	0,123906
P1	0,624032	0,648819	0,72111	0,550829	0,533212	0,523003	0,50169	0,501399	0,494212	0,4797	0,428173	0,444064
P2	0,458523	0,482858	0,521791	0,749206	0,712572	0,74329	0,530765	0,517203	0,494495	0,499648	0,459358	0,471543
P3	0,427078	0,439428	0,463606	0,533666	0,512792	0,509693	0,731204	0,713533	0,725873	0,506357	0,467567	0,478149

NBC-News - G16B7-QP=10		
	I	**P1**
B1	0,683626	0,744208
B2	0,663164	0,773117
B3	0,633941	0,798962
B4	0,663278	0,808204
B5	0,621925	0,827254
B6	0,650271	0,814179
B7	0,637682	0,815341
B8	0,628923	0,745809
B9	0,609686	0,755634
B10	0,590452	0,741746
B11	0,625761	0,72935
B12	0,578254	0,717658
B13	0,60322	0,699509
B14	0,601146	0,679077

NBC-News - G16B7-QP=28		
	I	**P1**
B1	0,087799	0,606916
B2	0,103772	0,69727
B3	0,096554	0,725786
B4	0,103905	0,739545
B5	0,105279	0,741712
B6	0,101581	0,711083
B7	0,084889	0,62944
B8	0,075489	0,585038
B9	0,087724	0,638198
B10	0,091648	0,643751
B11	0,101307	0,634164
B12	0,090272	0,608186
B13	0,078433	0,567489
B14	0,068066	0,497746

NBC-News - G16B7-QP=48		
	I	**P1**
B1	-0,11677	0,601495
B2	-0,13263	0,623131
B3	-0,13953	0,638485
B4	-0,14607	0,643108
B5	-0,13979	0,637401
B6	-0,14153	0,610887
B7	-0,13061	0,567944
B8	-0,13072	0,461908
B9	-0,12174	0,464087
B10	-0,12589	0,476302
B11	-0,12993	0,465456
B12	-0,12438	0,458982
B13	-0,11482	0,421585
B14	-0,11589	0,385588

Silence of the Lambs - G16B15-QP=10	
	I
B1	0,577297
B2	0,696233
B3	0,692309
B4	0,694009
B5	0,694725
B6	0,691289
B7	0,6903
B8	0,689233
B9	0,688639
B10	0,688496
B11	0,693083
B12	0,693069
B13	0,693198
B14	0,688871
B15	0,569106

Star Wars IV - G16B15-QP=28	
	I
B1	0,222495
B2	0,26699
B3	0,283271
B4	0,283432
B5	0,285077
B6	0,285536
B7	0,28768
B8	0,285774
B9	0,291468
B10	0,292644
B11	0,286469
B12	0,278039
B13	0,266525
B14	0,248834
B15	0,208514

NBC-News - G16B15-QP=48	
	I
B1	-0,11674
B2	-0,13467
B3	-0,14604
B4	-0,15529
B5	-0,14201
B6	-0,13972
B7	-0,13519
B8	-0,13303
B9	-0,13311
B10	-0,13037
B11	-0,13378
B12	-0,1372
B13	-0,13036
B14	-0,11815
B15	-0,11467

Silence of the Lambs

Autocorrelation B-frames

	B1(frames/gop)			B3(frames/gop)			B7(frames/gop)			B15(frames/gop)		
lag	Qp=10	Qp=28	Qp=48	Qp=10	Qp=28	Qp=48	Qp=10	Qp=28	Qp=48	Qp=10	Qp=28	Qp=48
1	0,168017	0,29691	0,57854	0,72491	0,79907	0,83691	0,8862	0,9214	0,9197	0,9497	0,9639	0,9554
2	0,36205	0,57519	0,56186	0,72273	0,75208	0,73289	0,84453	0,85129	0,8429	0,9207	0,9212	0.9092
16	0,21403	0,34004	0,32597	0,71569	0,73069	0,55009	0,7954	0,7894	0,6597	0,8866	0,8785	0,7495
20	0,511634	0,661152	0,32767	0,68356	0,71701	0,50570	0,8135	0,8201	0,6400	0,8165	0,7666	0,6430
32	0,30576	0,43041	0,23482	0,62555	0,65035	0,41803	0,7477	0,7201	0,5211	0,8286	0,8037	0,6146
40	0,44788	0,50624	0,20112	0,62124	0,65055	0,36685	0,7386	0,7208	0,4777	0,7698	0,7158	0,5185
48	0,44595	0,41418	0,16925	0,61231	0,62681	0,31176	0,7607	0,7550	0,4447	0,7750	0,7327	0,5040
60	0,571351	0,43019	0,145119	0,64960	0,65677	0,25814	0,6895	0,6519	0,3592	0,7904	0,7586	0,4686
64	0,24703	0,29021	0,10653	0,60799	0,61830	0,24131	0,7155	0,6982	0,3600	0,7272	0,6724	0,4150
80	0,371491	0,34160	0,12488	0,56094	0,55194	0,17510	0,6513	0,6027	0,2661	0,6866	0,6203	0,3343
96	0,26755	0,34642	0,110079	0,53925	0,50703	0,14797	0,6425	0,5935	0,2182	0,6536	0,5729	0,2733
100	0,33695	0,28568	0,10694	0,52920	0,49598	0,14772	0,6301	0,5739	0,2122	0,6534	0,5774	0,2688
112	0,28048	0,217812	0,10436	0,51690	0,48023	0,13054	0,6524	0,6008	0,1920	0,6268	0,5384	0,2308
128	0,30840	0,26039	0,10475	0,51951	0,46645	0,12092	0,6011	0,5370	0,1694	0,6076	0,5145	0,2012
144	0,20295	0,16274	0,08558	0,52942	0,48900	0,12413	0,5731	0,4930	0,1482	0,5952	0,5010	0,1841
160	0,25770	0,15249	0,07680	0,47633	0,41401	0,10678	0,5958	0,5175	0,1518	0,5869	0,4905	0,1705
176	0,21875	0,14496	0,06313	0,47277	0,39405	0,10612	0,5894	0,5031	0,1465	0,5842	0,4902	0,1689
192	0,22828	0,10235	0,05629	0,45976	0,35703	0,10611	0,5328	0,4349	0,1229	0,5843	0,4897	0,1657
200	0,23957	0,12824	0,04649	0,44739	0,34964	0,10683	0,5266	0,4246	0,1197	0,5550	0,4479	0,1533
208	0,20533	0,111214	0,03916	0,43430	0,31763	0,09853	0,5296	0,4240	0,1275	0,5866	0,4913	0,1655
224	0,161771	0,08359	0,03953	0,41288	0,27006	0,10331	0,5541	0,4328	0,1375	0,5919	0,4835	0,1715
240	0,25955	0,12248	0,05989	0,43229	0,26169	0,09167	0,4992	0,3575	0,1259	0,5833	0,4624	0,1776
256	0,17531	0,09799	0,06098	0,38315	0,22539	0,07562	0,4768	0,3120	0,1208	0,5633	0,4265	0,1708
272	0,16479	0,09805	0,06124	0,37205	0,19718	0,07069	0,4965	0,3205	0,1176	0,5369	0,3868	0,1555
288	0,20124	0,12366	0,06253	0,39359	0,19193	0,06287	0,4818	0,2946	0,1099	0,5066	0,3412	0,1382
304	0,1663	0,12894	0,04617	0,37320	0,17920	0,03272	0,4354	0,2338	0,0854	0,4805	0,2977	0,1232
320	0,18028	0,15828	0,05143	0,34879	0,17076	0,03025	0,4362	0,2285	0,0715	0,4576	0,2641	0,1063

lag	Qp=10	Qp=28	Qp=48	Qp=10	Qp=28	Qp=48	Qp=10	Qp=28	Qp=48	Qp=10	Qp=28	Qp=48
336	0,162781	0,15109	0,03462	0,35282	0,16919	0,05672	0,4720	0,2457	0,0638	0,4411	0,2382	0,0897
352	0,16927	0,146881	0,04289	0,33484	0,16231	0,08075	0,4176	0,2030	0,0353	0,4288	0,2175	0,0710
368	0,18420	0,157797	0,07042	0,33256	0,16447	0,07342	0,3961	0,1801	0,0254	0,4209	0,2043	0,0469
384	0,163012	0,156416	0,09052	0,34931	0,17599	0,06777	0,4236	0,2092	0,0443	0,4143	0,2009	0,0376
400	0,18223	0,16046	0,08745	0,31872	0,16868	0,06700	0,4193	0,2117	0,0613	0,4122	0,1998	0,0411
416	0,16955	0,15706	0,08722	0,32284	0,17537	0,07207	0,3778	0,1759	0,0772	0,4135	0,2075	0,0515
432	0,18876	0,14033	0,10073	0,32997	0,18735	0,06937	0,3855	0,1892	0,0690	0,4211	0,2215	0,0682
448	0,18093	0,15642	0,10372	0,30108	0,19549	0,06637	0,4214	0,2208	0,0678	0,4329	0,2370	0,0817
464	0,16646	0,141759	0,112638	0,29024	0,20536	0,05741	0,3745	0,1887	0,0613	0,4470	0,2491	0,0825
480	0,20715	0,14434	0,12076	0,31791	0,22578	0,05224	0,3559	0,1818	0,0669	0,4466	0,2513	0,0807
496	0,195071	0,131762	0,09422	0,28892	0,21871	0,03798	0,3827	0,2183	0,0741	0,4306	0,2446	0,0749
512	0,179419	0,10347	0,101364	0,28764	0,22374	0,03958	0,3777	0,2215	0,0758	0,4050	0,2310	0,0723
528	0,16878	0,09541	0,09003	0,30101	0,22724	0,04187	0,3319	0,1958	0,0624	0,3802	0,2136	0,0704
544	0,17882	0,091213	0,110704	0,29402	0,22812	0,06198	0,3347	0,2114	0,0618	0,3604	0,2022	0,0696
560	0,16844	0,09835	0,117832	0,29301	0,23011	0,08686	0,3760	0,2459	0,0523	0,3438	0,1926	0,0576
576	0,163019	0,07745	0,09439	0,31454	0,23881	0,11069	0,3304	0,2171	0,0343	0,3284	0,1826	0,0450
592	0,17266	0,06427	0,08300	0,29351	0,22120	0,12463	0,3192	0,2111	0,0354	0,3202	0,1798	0,0322
608	0,15184	0,05753	0,07085	0,29088	0,22107	0,12904	0,3560	0,2491	0,0418	0,3173	0,1798	0,0213
624	0,16457	0,04190	0,06635	0,31661	0,23134	0,12808	0,3537	0,2511	0,0563	0,3195	0,1878	0,0166
640	0,177783	0,04398	0,06540	0,29855	0,21585	0,12136	0,3203	0,2209	0,0684	0,3237	0,1991	0,0254
656	0,165218	0,03534	0,04319	0,30603	0,21984	0,12197	0,3322	0,2350	0,0887	0,3312	0,2094	0,0345
672	0,16374	0,02883	0,03593	0,32072	0,21865	0,12783	0,3721	0,2632	0,1139	0,3439	0,2259	0,0578
688	0,158917	0,02869	0,02258	0,30292	0,21209	0,12886	0,3295	0,2320	0,1191	0,3582	0,2411	0,0750
704	0,18044	0,03010	0,0272	0,30742	0,21013	0,13980	0,3196	0,2161	0,1191	0,3754	0,2536	0,0890
720	0,16002	0,019251	0,02542	0,34088	0,21857	0,14151	0,3563	0,2481	0,1378	0,3845	0,2578	0,1137
736	0,158197	0,018517	0,02840	0,31204	0,18888	0,13685	0,3616	0,2470	0,1387	0,3743	0,2544	0,1269
752	0,18733	0,01825	0,017918	0,31192	0,17708	0,11792	0,3302	0,2110	0,1307	0,3569	0,2420	0,1300
768	0,167651	0,01979	0,01623	0,32578	0,17053	0,11419	0,3454	0,2237	0,1254	0,3474	0,2349	0,1344
784	0,143101	0,01528	0,02257	0,30269	0,15633	0,11443	0,3857	0,2519	0,1347	0,3415	0,2223	0,1295
800	0,16969	0,017691	0,03415	0,30371	0,15186	0,14008	0,3477	0,2223	0,1379	0,3378	0,2140	0,1281

lag	Qp=10	Qp=28	Qp=48	Qp=10	Qp=28	Qp=48	Qp=10	Qp=28	Qp=48	Qp=10	Qp=28	Qp=48
816	0,13849	0,01145	0,02226	0,31664	0,14769	0,15666	0,3397	0,2099	0,1377	0,3384	0,2100	0,1217
832	0,143318	0,00873	0,01299	0,28943	0,12960	0,16640	0,3788	0,2432	0,1508	0,3386	0,2062	0,1152
848	0,141957	0,00786	0,01806	0,27786	0,12360	0,15234	0,3844	0,2370	0,1494	0,3393	0,2088	0,1186
864	0,13465	0,00974	0,01439	0,29896	0,12650	0,13841	0,3513	0,1978	0,1309	0,3441	0,2158	0,1212
880	0,136551	0,01239	0,02996	0,28167	0,10719	0,10814	0,3621	0,2019	0,1207	0,3534	0,2265	0,1291
896	0,122715	0,01105	0,04298	0,27706	0,09494	0,09707	0,3994	0,2252	0,1283	0,3693	0,2422	0,1359
912	0,13462	0,01476	0,04900	0,29462	0,09273	0,08582	0,3542	0,1875	0,1268	0,3877	0,2561	0,1359
928	0,111805	0,00557	0,02961	0,27871	0,07860	0,07413	0,3398	0,1697	0,1458	0,4071	0,2709	0,1333
944	0,12904	0,00751	0,01706	0,28199	0,07186	0,06893	0,3702	0,1963	0,1739	0,4245	0,2799	0,1337
960	0,13495	0,011086	0,016717	0,30613	0,07256	0,05863	0,3636	0,1915	0,1811	0,4310	0,2825	0,1396
976	0,111151	0,00748	0,011214	0,28273	0,06065	0,04486	0,3248	0,1525	0,1609	0,4184	0,2748	0,1529
992	0,13665	0,01514	0,02223	0,28382	0,05762	0,03638	0,3312	0,1564	0,1543	0,3975	0,2605	0,1759
1000	0,12965	0,01394	0,01595	0,28613	0,05774	0,03090	0,3554	0,1751	0,1476	0,3598	0,2154	0,1699

NBC NEWS												
Autocorrelation B-frames												
	B1(frames/gop)			B3(frames/gop)			B7(frames/gop)			B15(frames/gop)		
lag	Qp=10	Qp=28	Qp=48	Qp=10	Qp=28	Qp=48	Qp=10	Qp=28	Qp=48	Qp=10	Qp=28	Qp=48
1	0,8978	0,7996	0,7360	0,9328	0,8731	0,8546	0,9413	0,9121	0,9040	0,9557	0,9423	0,9371
2	0,8705	0,7604	0,5853	0,9035	0,8156	0,7491	0,9069	0,8355	0,8065	0,9248	0,8840	0,8691
16	0,6621	0,4560	0,2299	0,7177	0,5488	0,3554	0,7299	0,5775	0,4521	0,7589	0,6516	0,5555
20	0,6423	0,4836	0,2195	0,6919	0,5087	0,3373	0,7125	0,5705	0,4409	0,7023	0,5405	0,4669
32	0,5781	0,4160	0,2041	0,6172	0,4574	0,2821	0,6268	0,4739	0,3471	0,6509	0,5369	0,4261
40	0,5490	0,4072	0,2160	0,5947	0,4362	0,2759	0,6010	0,4572	0,3248	0,5950	0,4491	0,3501
48	0,5292	0,3817	0,1926	0,5666	0,4320	0,2686	0,5871	0,4671	0,3302	0,5792	0,4521	0,3458
60	0,5017	0,3695	0,2072	0,5304	0,4092	0,2793	0,5329	0,3965	0,2911	0,5613	0,4682	0,3414
64	0,4812	0,3225	0,1724	0,5133	0,3813	0,2379	0,5373	0,4183	0,3067	0,5232	0,3943	0,2991
80	0,4510	0,3137	0,1533	0,4946	0,3647	0,2703	0,4833	0,3425	0,2668	0,4769	0,3363	0,2812
96	0,4200	0,2949	0,1603	0,4614	0,3412	0,2390	0,4750	0,3553	0,3024	0,4532	0,3088	0,2795
100	0,4181	0,2732	0,1308	0,4522	0,3273	0,2251	0,4640	0,3427	0,2931	0,4512	0,3157	0,2857
112	0,3974	0,2728	0,1360	0,4371	0,3192	0,2193	0,4554	0,3594	0,2887	0,4256	0,2919	0,2715
128	0,3974	0,2750	0,1205	0,4069	0,3194	0,2165	0,4235	0,3211	0,2567	0,3988	0,2716	0,2451
144	0,3740	0,2467	0,1163	0,3926	0,3041	0,2048	0,3905	0,2887	0,2352	0,3771	0,2540	0,2351
160	0,3638	0,2312	0,1075	0,3632	0,2763	0,1765	0,3858	0,3033	0,2376	0,3592	0,2542	0,2228
176	0,3500	0,2467	0,1155	0,3606	0,2739	0,1850	0,3693	0,2957	0,2099	0,3490	0,2538	0,2175
192	0,3329	0,1950	0,0977	0,3684	0,2874	0,1791	0,3426	0,2569	0,2035	0,3368	0,2544	0,2116
200	0,3262	0,1811	0,0989	0,3612	0,2812	0,1835	0,3429	0,2546	0,2014	0,3217	0,2259	0,1880
208	0,3145	0,1894	0,1088	0,3560	0,2768	0,1859	0,3465	0,2576	0,2112	0,3385	0,2727	0,2301
224	0,3084	0,2161	0,0995	0,3482	0,2577	0,1681	0,3650	0,2987	0,2228	0,3436	0,2771	0,2318
240	0,2895	0,1663	0,0718	0,3362	0,2558	0,1575	0,3430	0,2619	0,2118	0,3506	0,2892	0,2216
256	0,2882	0,1872	0,1031	0,3201	0,2402	0,1603	0,3269	0,2384	0,1911	0,3424	0,2824	0,2261
272	0,2810	0,1824	0,0899	0,3130	0,2308	0,1521	0,3328	0,2669	0,2006	0,3234	0,2532	0,2051
288	0,2639	0,1478	0,0870	0,3082	0,2221	0,1459	0,3209	0,2513	0,1884	0,3092	0,2328	0,1957
304	0,2736	0,1906	0,1032	0,2898	0,2024	0,1474	0,2983	0,2045	0,1682	0,2942	0,2098	0,1836
320	0,2613	0,1724	0,0778	0,2825	0,2183	0,1530	0,3007	0,2174	0,1819	0,2806	0,1832	0,1685

lag	Qp=10	Qp=28	Qp=48	Qp=10	Qp=28	Qp=48	Qp=10	Qp=28	Qp=48	Qp=10	Qp=28	Qp=48
336	0,2491	0,1560	0,0625	0,2809	0,2259	0,1457	0,3056	0,2357	0,1855	0,2694	0,1620	0,1616
352	0,2417	0,1811	0,0597	0,2691	0,1904	0,1125	0,2782	0,1985	0,1628	0,2665	0,1561	0,1626
368	0,2291	0,1612	0,0638	0,2634	0,1855	0,1287	0,2603	0,1850	0,1722	0,2518	0,1450	0,1558
384	0,2263	0,1750	0,0961	0,2651	0,2015	0,1438	0,2710	0,2096	0,1681	0,2419	0,1408	0,1621
400	0,2200	0,2003	0,0728	0,2538	0,1884	0,1293	0,2661	0,2075	0,1562	0,2350	0,1481	0,1719
416	0,1884	0,1562	0,0539	0,2481	0,1760	0,1391	0,2527	0,1697	0,1425	0,2362	0,1565	0,1609
432	0,1964	0,1888	0,0690	0,2400	0,1651	0,1271	0,2528	0,1702	0,1490	0,2444	0,1723	0,1583
448	0,1880	0,1826	0,0746	0,2396	0,1697	0,1261	0,2632	0,2015	0,1730	0,2484	0,1776	0,1657
464	0,1839	0,1642	0,0778	0,2444	0,1896	0,1200	0,2417	0,1631	0,1514	0,2547	0,1869	0,1836
480	0,1937	0,1881	0,0570	0,2396	0,1859	0,1195	0,2318	0,1518	0,1484	0,2511	0,1918	0,1985
496	0,1840	0,1731	0,0603	0,2280	0,1770	0,1130	0,2345	0,1637	0,1567	0,2459	0,1822	0,1877
512	0,1783	0,1444	0,0542	0,2151	0,1623	0,1141	0,2332	0,1637	0,1549	0,2303	0,1573	0,1741
528	0,1719	0,1628	0,0440	0,2152	0,1723	0,1076	0,2250	0,1465	0,1483	0,2143	0,1314	0,1556
544	0,1553	0,1120	0,0494	0,2047	0,1579	0,1130	0,2312	0,1626	0,1397	0,2027	0,1077	0,1393
560	0,1404	0,0852	0,0382	0,2039	0,1682	0,1165	0,2395	0,1875	0,1516	0,2056	0,1084	0,1436
576	0,1487	0,1184	0,0319	0,2011	0,1786	0,1467	0,2156	0,1532	0,1358	0,2071	0,1132	0,1407
592	0,1553	0,0883	0,0195	0,1902	0,1865	0,1191	0,2018	0,1379	0,1272	0,2012	0,1096	0,1332
608	0,1547	0,1085	0,0288	0,1754	0,1597	0,1009	0,2070	0,1523	0,1352	0,1936	0,1039	0,1218
624	0,1519	0,1260	0,0208	0,1592	0,1627	0,1028	0,2037	0,1504	0,1502	0,1902	0,1079	0,1263
640	0,1490	0,1174	0,0426	0,1531	0,1571	0,1088	0,1859	0,1276	0,1371	0,1802	0,0925	0,1163
656	0,1587	0,1371	0,0407	0,1623	0,1761	0,1280	0,1941	0,1467	0,1474	0,1809	0,0969	0,1239
672	0,1555	0,1200	0,0491	0,1572	0,1749	0,1210	0,2001	0,1758	0,1764	0,1836	0,1136	0,1501
688	0,1574	0,1161	0,0541	0,1505	0,1527	0,1103	0,1784	0,1524	0,1451	0,1866	0,1348	0,1677
704	0,1509	0,1585	0,0505	0,1545	0,1681	0,1120	0,1609	0,1210	0,1184	0,1952	0,1548	0,1824
720	0,1396	0,1356	0,0503	0,1674	0,1843	0,1064	0,1581	0,1418	0,1274	0,1919	0,1657	0,1943
736	0,1336	0,1298	0,0391	0,1631	0,1786	0,1079	0,1457	0,1429	0,1240	0,1807	0,1612	0,1726
752	0,1506	0,1846	0,0641	0,1530	0,1536	0,0980	0,1373	0,1204	0,1310	0,1618	0,1274	0,1502
768	0,1314	0,1361	0,0462	0,1570	0,1570	0,0994	0,1447	0,1286	0,1463	0,1402	0,1055	0,1357
784	0,1131	0,1133	0,0406	0,1500	0,1393	0,0798	0,1568	0,1585	0,1534	0,1222	0,0876	0,1204
800	0,1100	0,1348	0,0330	0,1395	0,1308	0,0643	0,1403	0,1204	0,1375	0,1182	0,0787	0,1252

lag	Qp=10	Qp=28	Qp=48	Qp=10	Qp=28	Qp=48	Qp=10	Qp=28	Qp=48	Qp=10	Qp=28	Qp=48
816	0,1130	0,1209	0,0381	0,1326	0,1197	0,0754	0,1339	0,1223	0,1340	0,1217	0,0805	0,1197
832	0,1244	0,1334	0,0318	0,1171	0,0957	0,0530	0,1537	0,1589	0,1339	0,1203	0,0708	0,1310
848	0,1330	0,1315	0,0399	0,1149	0,0876	0,0558	0,1597	0,1518	0,1244	0,1179	0,0704	0,1253
864	0,1285	0,1123	0,0231	0,1282	0,1097	0,0459	0,1445	0,1290	0,1193	0,1156	0,0705	0,1289
880	0,1269	0,1331	0,0145	0,1316	0,0950	0,0421	0,1489	0,1368	0,1095	0,1244	0,0889	0,1303
896	0,1302	0,1026	0,0079	0,1358	0,1005	0,0471	0,1599	0,1519	0,1221	0,1331	0,1063	0,1224
912	0,1288	0,0910	0,0106	0,1391	0,1155	0,0485	0,1428	0,1154	0,0867	0,1446	0,1241	0,1272
928	0,1229	0,1290	0,0301	0,1328	0,1220	0,0495	0,1292	0,0991	0,0749	0,1497	0,1390	0,1273
944	0,1112	0,0708	0,0164	0,1299	0,1119	0,0472	0,1327	0,1114	0,0829	0,1552	0,1426	0,1155
960	0,1063	0,0500	-0,0048	0,1320	0,1318	0,0675	0,1271	0,1138	0,0820	0,1594	0,1447	0,1156
976	0,1041	0,0556	0,0057	0,1322	0,1143	0,0638	0,1052	0,0675	0,0550	0,1524	0,1301	0,1026
992	0,1129	0,0265	-0,0078	0,1386	0,1320	0,0677	0,1088	0,0663	0,0595	0,1345	0,1023	0,0886
1000	0,1137	0,0257	-0,0073	0,1343	0,1236	0,0643	0,1182	0,0830	0,0614	0,1157	0,0585	0,0568

STAR WARS IV												
Autocorrelation B-frames												
	B1(frames/gop)			B3(frames/gop)			B7(frames/gop)			B15(frames/gop)		
lag	Qp=10	Qp=28	Qp=48	Qp=10	Qp=28	Qp=48	Qp=10	Qp=28	Qp=48	Qp=10	Qp=28	Qp=48
1	0,6087	0,6782	0,5776	0,8424	0,8555	0,8098	0,9156	0,9165	0,9020	0,9521	0,9531	0,9449
2	0,6032	0,6507	0,5262	0,8129	0,8031	0,7002	0,8554	0,8259	0,8190	0,9029	0,8949	0,8964
16	0,4457	0,3862	0,1793	0,6374	0,5494	0,3569	0,6843	0,5968	0,4822	0,7665	0,7095	0,5937
20	0,4564	0,3485	0,1486	0,6124	0,5068	0,3304	0,6857	0,6016	0,4462	0,6354	0,5574	0,5095
32	0,3839	0,2871	0,1241	0,5189	0,3968	0,2500	0,5592	0,4350	0,3518	0,6296	0,5467	0,4494
40	0,3029	0,2673	0,1012	0,4722	0,3598	0,2359	0,5246	0,4059	0,3186	0,5141	0,4162	0,3772
48	0,2777	0,2515	0,0777	0,4495	0,3545	0,2091	0,5170	0,4156	0,3062	0,5203	0,4312	0,3700
60	0,2391	0,2147	0,0811	0,4091	0,3377	0,1800	0,4264	0,3254	0,2599	0,5408	0,4563	0,3412
64	0,2418	0,2221	0,0900	0,3860	0,3155	0,1703	0,4595	0,3764	0,2662	0,4388	0,3627	0,3124
80	0,2024	0,1657	0,0754	0,3400	0,2880	0,1655	0,3720	0,3024	0,2329	0,3744	0,3139	0,2824
96	0,1946	0,1314	0,0561	0,3190	0,2809	0,1588	0,3501	0,2967	0,2161	0,3259	0,2755	0,2526
100	0,1909	0,1251	0,0481	0,2967	0,2509	0,1523	0,3435	0,2926	0,2119	0,3305	0,2810	0,2503
112	0,1874	0,1186	0,0301	0,2776	0,2342	0,1381	0,3670	0,3280	0,2155	0,2885	0,2471	0,2339
128	0,1624	0,1053	0,0327	0,2611	0,1983	0,1193	0,2972	0,2513	0,1791	0,2625	0,2213	0,2091
144	0,1575	0,1154	0,0623	0,2643	0,1907	0,1083	0,2608	0,2016	0,1662	0,2566	0,2138	0,1988
160	0,1503	0,1103	0,0576	0,2421	0,1626	0,0873	0,2963	0,2324	0,1518	0,2546	0,2031	0,1864
176	0,1376	0,0995	0,0418	0,2347	0,1539	0,0749	0,2901	0,2191	0,1367	0,2684	0,2092	0,1721
192	0,1294	0,0908	0,0314	0,2235	0,1525	0,0631	0,2378	0,1602	0,1053	0,2857	0,2201	0,1560
200	0,1424	0,1058	0,0362	0,2055	0,1417	0,0756	0,2354	0,1597	0,1061	0,2370	0,1743	0,1389
208	0,1296	0,1015	0,0328	0,2029	0,1472	0,0820	0,2460	0,1721	0,1038	0,3028	0,2320	0,1386
224	0,1185	0,0835	0,0350	0,2000	0,1483	0,0805	0,2705	0,2055	0,1025	0,3171	0,2459	0,1505
240	0,1051	0,0811	0,0409	0,2028	0,1549	0,0895	0,2160	0,1611	0,1013	0,3136	0,2444	0,1474
256	0,0959	0,0669	0,0210	0,1890	0,1437	0,0719	0,1936	0,1414	0,1043	0,2938	0,2326	0,1378
272	0,0919	0,0573	0,0107	0,1829	0,1328	0,0598	0,2356	0,1932	0,1141	0,2648	0,2137	0,1318
288	0,0980	0,0668	0,0287	0,1815	0,1358	0,0693	0,2294	0,1859	0,1051	0,2354	0,1914	0,1367
304	0,0952	0,0667	0,0306	0,1739	0,1376	0,0654	0,1839	0,1374	0,0896	0,2112	0,1679	0,1343
320	0,0741	0,0566	0,0365	0,1658	0,1233	0,0737	0,1965	0,1523	0,0827	0,1896	0,1512	0,1216

lag	Qp=10	Qp=28	Qp=48	Qp=10	Qp=28	Qp=48	Qp=10	Qp=28	Qp=48	Qp=10	Qp=28	Qp=48
336	0,0521	0,0284	0,0299	0,1663	0,1258	0,0663	0,2283	0,1882	0,0914	0,1732	0,1314	0,1131
352	0,0496	0,0336	0,0269	0,1435	0,1108	0,0720	0,1850	0,1492	0,0969	0,1556	0,1167	0,1084
368	0,0401	0,0322	0,0356	0,1309	0,0981	0,0521	0,1651	0,1241	0,0973	0,1517	0,1159	0,1159
384	0,0300	0,0302	0,0306	0,1362	0,0994	0,0471	0,2002	0,1611	0,0924	0,1573	0,1238	0,1274
400	0,0340	0,0390	0,0200	0,1226	0,0805	0,0299	0,1944	0,1543	0,0988	0,1667	0,1271	0,1257
416	0,0240	0,0345	0,0069	0,1245	0,0860	0,0423	0,1373	0,1027	0,0865	0,1764	0,1381	0,1166
432	0,0284	0,0444	-0,0023	0,1399	0,1007	0,0591	0,1428	0,1070	0,0719	0,1936	0,1505	0,1248
448	0,0208	0,0386	-0,0088	0,1288	0,0986	0,0589	0,1840	0,1410	0,0719	0,2085	0,1661	0,1246
464	0,0146	0,0265	-0,0004	0,1159	0,0819	0,0565	0,1368	0,0886	0,0468	0,2254	0,1745	0,1097
480	0,0086	0,0136	-0,0075	0,1115	0,0835	0,0612	0,1252	0,0804	0,0594	0,2343	0,1746	0,1010
496	-0,0079	-0,0006	-0,0116	0,0821	0,0508	0,0548	0,1723	0,1334	0,0747	0,2198	0,1588	0,0873
512	0,0014	0,0196	-0,0055	0,0730	0,0401	0,0414	0,1710	0,1361	0,0899	0,2001	0,1513	0,0997
528	-0,0119	0,0126	0,0069	0,0846	0,0601	0,0549	0,1229	0,0890	0,0792	0,1739	0,1370	0,1035
544	-0,0140	0,0008	0,0012	0,0698	0,0567	0,0587	0,1274	0,0956	0,0754	0,1509	0,1230	0,1133
560	-0,0154	0,0044	0,0135	0,0675	0,0549	0,0562	0,1595	0,1303	0,0722	0,1290	0,1069	0,1037
576	-0,0033	0,0235	0,0318	0,0653	0,0613	0,0548	0,0970	0,0662	0,0556	0,1104	0,0884	0,0961
592	-0,0088	0,0211	0,0402	0,0457	0,0491	0,0430	0,0755	0,0427	0,0485	0,0920	0,0740	0,0892
608	-0,0040	0,0276	0,0544	0,0460	0,0496	0,0257	0,1159	0,0875	0,0637	0,0840	0,0678	0,0798
624	-0,0073	0,0338	0,0284	0,0483	0,0555	0,0218	0,1147	0,0940	0,0677	0,0761	0,0621	0,0761
640	-0,0319	0,0108	0,0271	0,0400	0,0555	0,0218	0,0690	0,0554	0,0756	0,0843	0,0666	0,0796
656	-0,0267	0,0162	0,0155	0,0393	0,0558	0,0236	0,0830	0,0718	0,0746	0,1063	0,0915	0,0985
672	-0,0145	0,0249	0,0411	0,0466	0,0657	0,0174	0,1141	0,1107	0,0674	0,1279	0,1166	0,1079
688	-0,0201	0,0079	0,0277	0,0358	0,0543	0,0168	0,0637	0,0643	0,0548	0,1485	0,1338	0,1080
704	-0,0085	0,0164	0,0262	0,0247	0,0357	0,0072	0,0412	0,0355	0,0393	0,1686	0,1508	0,1043
720	0,0021	0,0140	0,0129	0,0230	0,0331	0,0053	0,0777	0,0803	0,0318	0,1707	0,1537	0,0920
736	0,0120	0,0304	0,0110	0,0013	0,0003	-0,0055	0,0746	0,0820	0,0333	0,1516	0,1410	0,0861
752	0,0081	0,0255	-0,0022	0,0009	0,0126	-0,0103	0,0361	0,0470	0,0351	0,1202	0,1133	0,0815
768	0,0217	0,0277	0,0031	0,0102	0,0330	0,0059	0,0505	0,0641	0,0291	0,0863	0,0889	0,0628
784	0,0222	0,0270	0,0097	-0,0034	0,0277	0,0119	0,0929	0,1093	0,0323	0,0627	0,0721	0,0578
800	0,0194	0,0471	0,0134	-0,0185	0,0139	0,0132	0,0500	0,0705	0,0225	0,0473	0,0627	0,0518

lag	Qp=10	Qp=28	Qp=48	Qp=10	Qp=28	Qp=48	Qp=10	Qp=28	Qp=48	Qp=10	Qp=28	Qp=48
816	0,0304	0,0587	0,0149	-0,0107	0,0101	0,0026	0,0238	0,0397	0,0140	0,0350	0,0490	0,0494
832	0,0371	0,0649	0,0046	-0,0096	0,0111	0,0130	0,0539	0,0647	0,0143	0,0261	0,0429	0,0374
848	0,0383	0,0543	0,0125	-0,0038	0,0201	0,0382	0,0454	0,0492	0,0047	0,0263	0,0485	0,0401
864	0,0424	0,0628	0,0185	0,0068	0,0391	0,0521	-0,0063	-0,0035	-0,0098	0,0303	0,0542	0,0352
880	0,0369	0,0761	0,0155	-0,0051	0,0303	0,0574	0,0177	0,0251	0,0027	0,0371	0,0563	0,0334
896	0,0512	0,0777	0,0153	-0,0072	0,0315	0,0662	0,0527	0,0702	0,0187	0,0493	0,0625	0,0274
912	0,0457	0,0583	0,0078	0,0056	0,0437	0,0750	0,0085	0,0394	0,0269	0,0600	0,0605	0,0163
928	0,0640	0,0613	0,0097	-0,0127	0,0366	0,0627	-0,0199	0,0092	0,0209	0,0791	0,0755	0,0162
944	0,0671	0,0598	0,0373	-0,0237	0,0302	0,0563	0,0173	0,0399	0,0151	0,1074	0,1044	0,0283
960	0,0791	0,0666	0,0356	-0,0290	0,0201	0,0506	0,0216	0,0383	0,0148	0,1104	0,1147	0,0356
976	0,0799	0,0632	0,0213	-0,0361	0,0071	0,0436	-0,0160	0,0047	0,0252	0,0943	0,1094	0,0482
992	0,0651	0,0521	0,0217	-0,0247	0,0176	0,0503	0,0083	0,0286	0,0383	0,0628	0,0863	0,0412
1000	0,0681	0,0585	0,0176	-0,0168	0,0271	0,0505	0,0356	0,0587	0,0488	-0,0107	0,0200	0,0198

APPENDIX B

In this Appendix we present the equation sets for the movies we studied along with the Tables with the results of α_j and γ_j.

NBC news-G16B1-QP=10

$$\hat{B}_{1,t} = a_1 P_{1,t} + \gamma_1 B_{8,t-1}$$
$$\hat{B}_{2,t} = a_2 P_{2,t} + \gamma_2 B_{1,t}$$
$$\hat{B}_{3,t} = a_3 P_{3,t} + \gamma_3 B_{2,t}$$
$$\hat{B}_{4,t} = a_4 P_{4,t} + \gamma_4 B_{3,t}$$
$$\hat{B}_{5,t} = a_5 P_{5,t} + \gamma_5 B_{4,t}$$
$$\hat{B}_{6,t} = a_6 P_{6,t} + \gamma_6 B_{5,t}$$
$$\hat{B}_{7,t} = a_7 P_{7,t} + \gamma_7 B_{6,t}$$
$$\hat{B}_{8,t} = a_8 B_{7,t} + \gamma_8 B_{6,t}$$

NBC news -G16B1-QP=10		
	α	**γ**
B-1	0,334024	0,484232
B-2	0,464268	0,34528
B-3	0,305404	0,526498
B-4	0,324973	0,497887
B-5	0,342938	0,468501
B-6	0,321915	0,500492
B-7	0,309038	0,521344
B-8	0,309464	0,692055

NBC news -G16B1-QP=28

$(B_{1,t})=a_1*B_{7,t-1}+\gamma_1*B_{8,t-1}$
$(B_{2,t})=a_2*B_{8,t-1}+\gamma_2*B_{1,t}$
$(B_{3,t})=a_3*B_{1,t}+\gamma_3*B_{2,t}$
$(B_{4,t})=a_4*B_{2,t}+\gamma_4*B_{3,t}$
$(B_{5,t})=a_5*B_{3,t}+\gamma_5*B_{4,t}$
$(B_{6,t})=a_6*B_{4,t}+\gamma_6*B_{5,t}$
$(B_{7,t})=a_7*B_{5,t}+\gamma_7*B_{6,t}$
$(B_{8,t})=a_8*B_{6,t}+\gamma_8*B_{7,t}$

NBC news -G16B1-QP=28		
	α	**γ**
B-1	0,087366	1,280545
B-2	0,127123	1,19216
B-3	0,164968	1,118517
B-4	0,39627	0,989896
B-5	0,080462	1,243065
B-6	0,335059	0,896904
B-7	0,297877	1,052111
B-8	0,594406	0,716133

NBC news -G16B1-QP=48

$(B_{1,t})=a_1*B_{8,t-1}+\gamma_1*P_{1,t}$
$(B_{2,t})=a_2*B_{1,t}+\gamma_2*P_{2,t}$
$(B_{3,t})=a_3*B_{2,t}+\gamma_3*P_{3,t}$
$(B_{4,t})=a_4*B_{3,t}+\gamma_4*P_{4,t}$
$(B_{5,t})=a_5*B_{4,t}+\gamma_5*P_{5,t}$
$(B_{6,t})=a_6*B_{5,t}+\gamma_6*P_{6,t}$
$(B_{7,t})=a_7*B_{6,t}+\gamma_7*P_{7,t}$
$(B_{8,t})=a_8*B_{7,t}+\gamma_8*B_{6,t}$

NBC news -G16B1-QP=48		
	α	**γ**
B-1	0,580066	0,072585
B-2	0,920062	0,015224
B-3	0,722454	0,068832
B-4	0,904419	0,021228
B-5	0,94285	0,011812
B-6	0,924457	0,016029
B-7	0,882669	0,026682
B-8	1,077669	-0,04186

NBC news -G16B3-QP=10

$(B_{1,t})=a_1*B_{11,t-1}+\gamma_1*B_{12,t-1}$
$(B_{2,t})=a_2*B_{12,t-1}+\gamma_2*B_{1,t}$
$(B_{3,t})=a_3*B_{1,t}+\gamma_3*B_{2,t}$
$(B_{4,t})=a_4*B_{2,t}+\gamma_4*B_{3,t}$
$(B_{5,t})=a_5*B_{3,t}+\gamma_5*B_{4,t}$
$(B_{6,t})=a_6*B_{4,t}+\gamma_6*B_{5,t}$
$(B_{7,t})=a_7*B_{5,t}+\gamma_7*B_{6,t}$
$(B_{8,t})=a_8*B_{6,t}+\gamma_8*B_{7,t}$
$(B_{9,t})=a_9*B_{7,t}+\gamma_9*B_{8,t}$
$(B_{10,t})=a_{10}*B_{8,t}+\gamma_{10}*B_{9,t}$
$(B_{11,t})=a_{11}*B_{9,t}+\gamma_{11}*B_{10,t}$
$(B_{12,t})=a_{12}*B_{10,t}+\gamma_{12}*B_{11,t}$

NBC news -G16B3-QP=10		
	α	**γ**
B-1	0,3800	0,6108
B-2	0,2322	0,8012
B-3	0,2240	0,7634
B-4	0,2551	0,7343
B-5	0,2016	0,8292
B-6	0,1819	0,8054
B-7	0,3008	0,6861
B-8	0,2507	0,7792
B-9	0,1314	0,8514
B-10	0,2661	0,7239
B-11	0,2073	0,8232
B-12	0,1688	0,8155

NBC news -G16B3-QP=28

$(B_{1,t})=a_1*B_{11,t-1}+\gamma_1*B_{12,t-1}$
$(B_{2,t})=a_2*B_{12,t-1}+\gamma_2*B_{1,t}$
$(B_{3,t})=a_3*B_{1,t}+\gamma_3*B_{2,t}$
$(B_{4,t})=a_4*B_{2,t}+\gamma_4*B_{3,t}$
$(B_{5,t})=a_5*B_{3,t}+\gamma_5*B_{4,t}$
$(B_{6,t})=a_6*B_{4,t}+\gamma_6*B_{5,t}$
$(B_{7,t})=a_7*B_{5,t}+\gamma_7*B_{6,t}$
$(B_{8,t})=a_8*B_{6,t}+\gamma_8*B_{7,t}$
$(B_{9,t})=a_9*B_{7,t}+\gamma_9*B_{8,t}$
$(B_{10,t})=a_{10}*B_{8,t}+\gamma_{10}*B_{9,t}$
$(B_{11,t})=a_{11}*B_{9,t}+\gamma_{11}*B_{10,t}$
$(B_{12,t})=a_{12}*B_{10,t}+\gamma_{12}*B_{11,t}$

NBC news -G16B3-QP=28		
	α	**γ**
B-1	0,030959	1,144627
B-2	0,064004	1,24741
B-3	0,596092	0,483236
B-4	0,043007	1,187245
B-5	0,041375	1,302964
B-6	0,259544	0,765142
B-7	0,033107	1,146467
B-8	0,039903	1,257669
B-9	0,011334	0,95825
B-10	0,022239	1,20438
B-11	0,36221	0,933577
B-12	0,556363	0,462025

NBC news -G16B3-QP=48

$(B_{1,t})=a_1*B_{11,t-1}+\gamma_1*B_{12,t-1}$
$(B_{2,t})=a_2*B_{12,t-1}+\gamma_2*B_{1,t}$
$(B_{3,t})=a_3*B_{1,t}+\gamma_3*B_{2,t}$
$(B_{4,t})=a_4*B_{2,t}+\gamma_4*B_{3,t}$
$(B_{5,t})=a_5*B_{3,t}+\gamma_5*B_{4,t}$
$(B_{6,t})=a_6*B_{4,t}+\gamma_6*B_{5,t}$
$(B_{7,t})=a_7*B_{5,t}+\gamma_7*B_{6,t}$
$(B_{8,t})=a_8*B_{6,t}+\gamma_8*B_{7,t}$
$(B_{9,t})=a_9*B_{7,t}+\gamma_9*B_{8,t}$
$(B_{10,t})=a_{10}*B_{8,t}+\gamma_{10}*B_{9,t}$
$(B_{11,t})=a_{11}*B_{9,t}+\gamma_{11}*B_{10,t}$
$(B_{12,t})=a_{12}*B_{10,t}+\gamma_{12}*B_{11,t}$

NBC news -G16B3-QP=48		
	α	**γ**
B-1	0,243476	0,820433
B-2	0,03435	1,052805
B-3	0,302645	0,672866
B-4	0,052955	1,01063
B-5	0,048194	1,040187
B-6	0,292406	0,692228
B-7	0,113099	0,951938
B-8	0,063459	1,033285
B-9	0,415069	0,570293
B-10	0,179878	0,887888
B-11	0,052318	1,038395
B-12	0,287032	0,684752

NBC news -G16B7-QP=10

$(B_{1,t})=a_1*B_{11,t-1}+\gamma_1*B_{12,t-1}$
$(B_{2,t})=a_2*B_{12,t-1}+\gamma_2*B_{1,t}$
$(B_{3,t})=a_3*B_{1,t}+\gamma_3*B_{2,t}$
$(B_{4,t})=a_4*B_{2,t}+\gamma_4*B_{3,t}$
$(B_{5,t})=a_5*B_{3,t}+\gamma_5*B_{4,t}$
$(B_{6,t})=a_6*B_{4,t}+\gamma_6*B_{5,t}$
$(B_{7,t})=a_7*B_{5,t}+\gamma_7*B_{6,t}$
$(B_{8,t})=a_8*B_{6,t}+\gamma_8*B_{7,t}$
$(B_{9,t})=a_9*B_{7,t}+\gamma_9*B_{8,t}$
$(B_{10,t})=a_{10}*B_{8,t}+\gamma_{10}*B_{9,t}$
$(B_{11,t})=a_{11}*B_{9,t}+\gamma_{11}*B_{10,t}$
$(B_{12,t})=a_{12}*B_{10,t}+\gamma_{12}*B_{11,t}$
$(B_{13,t})=a_{13}*B_{11,t}+\gamma_{13}*B_{12,t}$
$(B_{14,t})=a_{14}*B_{12,t}+\gamma_{14}*B_{13,t}$

NBC news -G16B7-QP=10		
	α	γ
B-1	0,341485	0,645704
B-2	0,249847	0,802613
B-3	0,157731	0,859848
B-4	0,198578	0,825176
B-5	0,271053	0,719111
B-6	0,242456	0,750805
B-7	0,140828	0,809272
B-8	0,253475	0,735199
B-9	0,254126	0,795251
B-10	0,082104	0,928345
B-11	0,200409	0,824881
B-12	0,29493	0,694243
B-13	0,192115	0,804597
B-14	0,133908	0,816393

NBC news -G16B7-QP=28

$(B_{1,t})=a_1*B_{11,t-1}+\gamma_1*B_{12,t-1}$
$(B_{2,t})=a_2*B_{12,t-1}+\gamma_2*B_{1,t}$
$(B_{3,t})=a_3*B_{1,t}+\gamma_3*B_{2,t}$
$(B_{4,t})=a_4*B_{2,t}+\gamma_4*B_{3,t}$
$(B_{5,t})=a_5*B_{3,t}+\gamma_5*B_{4,t}$
$(B_{6,t})=a_6*B_{4,t}+\gamma_6*B_{5,t}$
$(B_{7,t})=a_7*B_{5,t}+\gamma_7*B_{6,t}$
$(B_{8,t})=a_8*B_{6,t}+\gamma_8*B_{7,t}$
$(B_{9,t})=a_9*B_{7,t}+\gamma_9*B_{8,t}$
$(B_{10,t})=a_{10}*B_{8,t}+\gamma_{10}*B_{9,t}$
$(B_{11,t})=a_{11}*B_{9,t}+\gamma_{11}*B_{10,t}$
$(B_{12,t})=a_{12}*B_{10,t}+\gamma_{12}*B_{11,t}$
$(B_{13,t})=a_{13}*B_{11,t}+\gamma_{13}*B_{12,t}$
$(B_{14,t})=a_{14}*B_{12,t}+\gamma_{14}*B_{13,t}$

NBC news -G16B7-QP=28		
	α	γ
B-1	0,042998	1,173432
B-2	0,261009	1,217924
B-3	0,194853	1,065181
B-4	0,298147	0,914796
B-5	0,008788	0,967551
B-6	0,082511	0,902098
B-7	0,28224	0,482585
B-8	0,108289	1,080027
B-9	0,04912	1,436071
B-10	-0,00221	1,142159
B-11	0,002525	1,148944
B-12	0,043585	0,933777
B-13	0,01598	0,984125
B-14	0,064503	0,735077

NBC news -G16B7-QP=48

$(B_{1,t})=a_1*B_{11,t-1}+\gamma_1*B_{12,t-1}$
$(B_{2,t})=a_2*B_{12,t-1}+\gamma_2*B_{1,t}$
$(B_{3,t})=a_3*B_{1,t}+\gamma_3*B_{2,t}$
$(B_{4,t})=a_4*B_{2,t}+\gamma_4*B_{3,t}$
$(B_{5,t})=a_5*B_{3,t}+\gamma_5*B_{4,t}$
$(B_{6,t})=a_6*B_{4,t}+\gamma_6*B_{5,t}$
$(B_{7,t})=a_7*B_{5,t}+\gamma_7*B_{6,t}$
$(B_{8,t})=a_8*B_{6,t}+\gamma_8*B_{7,t}$
$(B_{9,t})=a_9*B_{7,t}+\gamma_9*B_{8,t}$
$(B_{10,t})=a_{10}*B_{8,t}+\gamma_{10}*B_{9,t}$
$(B_{11,t})=a_{11}*B_{9,t}+\gamma_{11}*B_{10,t}$
$(B_{12,t})=a_{12}*B_{10,t}+\gamma_{12}*B_{11,t}$
$(B_{13,t})=a_{13}*B_{11,t}+\gamma_{13}*B_{12,t}$
$(B_{14,t})=a_{14}*B_{12,t}+\gamma_{14}*B_{13,t}$

NBC news -G16B7-QP=48		
	α	γ
B-1	0,171887	0,916521
B-2	0,057794	1,087378
B-3	0,076715	0,9936
B-4	0,048121	0,979079
B-5	0,344613	0,665917
B-6	0,104543	0,880349
B-7	0,026325	0,92223
B-8	0,12243	0,93805
B-9	0,155334	0,999957
B-10	0,088875	0,98139
B-11	0,165616	0,856229
B-12	0,314739	0,699514
B-13	0,104856	0,888201
B-14	0,063366	0,86455

NBC news -G16B15-QP=10

$(B_{1,t})=a_1*B_{11,t-1}+\gamma_1*B_{12,t-1}$
$(B_{2,t})=a_2*B_{12,t-1}+\gamma_2*B_{1,t}$
$(B_{3,t})=a_3*B_{1,t}+\gamma_3*B_{2,t}$
$(B_{4,t})=a_4*B_{2,t}+\gamma_4*B_{3,t}$
$(B_{5,t})=a_5*B_{3,t}+\gamma_5*B_{4,t}$
$(B_{6,t})=a_6*B_{4,t}+\gamma_6*B_{5,t}$
$(B_{7,t})=a_7*B_{5,t}+\gamma_7*B_{6,t}$
$(B_{8,t})=a_8*B_{6,t}+\gamma_8*B_{7,t}$
$(B_{9,t})=a_9*B_{7,t}+\gamma_9*B_{8,t}$
$(B_{10,t})=a_{10}*B_{8,t}+\gamma_{10}*B_{9,t}$
$(B_{11,t})=a_{11}*B_{9,t}+\gamma_{11}*B_{10,t}$
$(B_{12,t})=a_{12}*B_{10,t}+\gamma_{12}*B_{11,t}$
$(B_{13,t})=a_{13}*B_{11,t}+\gamma_{13}*B_{12,t}$
$(B_{14,t})=a_{14}*B_{12,t}+\gamma_{14}*B_{13,t}$
$(B_{15,t})=a_{15}*B_{13,t}+\gamma_{15}*B_{14,t}$

NBC news -G16B15-QP=10		
	α	γ
B-1	0,366834	0,614134
B-2	0,244027	0,821845
B-3	0,185392	0,848956
B-4	0,167587	0,854853
B-5	0,192692	0,814936
B-6	0,143435	0,861115
B-7	0,15453	0,856986
B-8	0,28821	0,715284
B-9	0,198557	0,80158
B-10	0,240012	0,758784
B-11	0,089615	0,900921
B-12	0,122192	0,881362
B-13	0,221054	0,761682
B-14	0,083006	0,896184
B-15	0,130915	0,811898

NBC news -G16B15-QP=28

$(B_{1,t})=a_1*B_{11,t-1}+\gamma_1*B_{12,t-1}$
$(B_{2,t})=a_2*B_{12,t-1}+\gamma_2*B_{1,t}$
$(B_{3,t})=a_3*B_{1,t}+\gamma_3*B_{2,t}$
$(B_{4,t})=a_4*B_{2,t}+\gamma_4*B_{3,t}$
$(B_{5,t})=a_5*B_{3,t}+\gamma_5*B_{4,t}$
$(B_{6,t})=a_6*B_{4,t}+\gamma_6*B_{5,t}$
$(B_{7,t})=a_7*B_{5,t}+\gamma_7*B_{6,t}$
$(B_{8,t})=a_8*B_{6,t}+\gamma_8*B_{7,t}$
$(B_{9,t})=a_9*B_{7,t}+\gamma_9*B_{8,t}$
$(B_{10,t})=a_{10}*B_{8,t}+\gamma_{10}*B_{9,t}$
$(B_{11,t})=a_{11}*B_{9,t}+\gamma_{11}*B_{10,t}$
$(B_{12,t})=a_{12}*B_{10,t}+\gamma_{12}*B_{11,t}$
$(B_{13,t})=a_{13}*B_{11,t}+\gamma_{13}*B_{12,t}$
$(B_{14,t})=a_{14}*B_{12,t}+\gamma_{14}*B_{13,t}$
$(B_{15,t})=a_{15}*B_{13,t}+\gamma_{15}*B_{14,t}$

NBC news -G16B15-QP=28		
	α	γ
B-1	0,060656	1,157423
B-2	0,14552	1,49642
B-3	0,204722	1,289318
B-4	0,710474	0,651944
B-5	0,049679	1,047679
B-6	0,040555	1,016834
B-7	0,00536	1,10028
B-8	0,032578	1,040592
B-9	0,100633	0,893308
B-10	0,00304	0,985846
B-11	-0,00062	1,000046
B-12	-0,00703	1,019345
B-13	0,074767	0,813784
B-14	0,000476	0,917227
B-15	0,000633	0,743123

NBC news -G16B15-QP=48

$(B_{1,t})=a_1*B_{11,t-1}+\gamma_1*B_{12,t-1}$
$(B_{2,t})=a_2*B_{12,t-1}+\gamma_2*B_{1,t}$
$(B_{3,t})=a_3*B_{1,t}+\gamma_3*B_{2,t}$
$(B_{4,t})=a_4*B_{2,t}+\gamma_4*B_{3,t}$
$(B_{5,t})=a_5*B_{3,t}+\gamma_5*B_{4,t}$
$(B_{6,t})=a_6*B_{4,t}+\gamma_6*B_{5,t}$
$(B_{7,t})=a_7*B_{5,t}+\gamma_7*B_{6,t}$
$(B_{8,t})=a_8*B_{6,t}+\gamma_8*B_{7,t}$
$(B_{9,t})=a_9*B_{7,t}+\gamma_9*B_{8,t}$
$(B_{10,t})=a_{10}*B_{8,t}+\gamma_{10}*B_{9,t}$
$(B_{11,t})=a_{11}*B_{9,t}+\gamma_{11}*B_{10,t}$
$(B_{12,t})=a_{12}*B_{10,t}+\gamma_{12}*B_{11,t}$
$(B_{13,t})=a_{13}*B_{11,t}+\gamma_{13}*B_{12,t}$
$(B_{14,t})=a_{14}*B_{12,t}+\gamma_{14}*B_{13,t}$
$(B_{15,t})=a_{15}*B_{13,t}+\gamma_{15}*B_{14,t}$

NBC news-G16B15-QP=48		
	α	γ
B-1	0,130076	0,960415
B-2	0,072625	1,1106
B-3	0,11812	0,994288
B-4	0,021736	1,058079
B-5	0,136166	0,922551
B-6	0,132939	0,907975
B-7	0,117418	0,927509
B-8	0,195677	0,819003
B-9	0,156981	0,849735
B-10	0,172805	0,830338
B-11	0,195247	0,800001
B-12	0,112268	0,872363
B-13	0,195367	0,77709
B-14	0,034544	0,929273
B-15	0,009523	0,901262

Star Wars IV-G16B1-QP=10

$(B_{1,t})=a_1*P_{1,t}+\gamma_1*B_{8,t-1}$
$(B_{2,t})=a_2*P_{2,t}+\gamma_2*P_{1,t}$
$(B_{3,t})=a_3*P_{3,t}+\gamma_3*P_{2,t}$
$(B_{4,t})=a_4*P_{4,t}+\gamma_4*P_{3,t}$
$(B_{5,t})=a_5*P_{5,t}+\gamma_5*P_{4,t}$
$(B_{6,t})=a_6*P_{6,t}+\gamma_6*P_{5,t}$
$(B_{7,t})=a_7*P_{7,t}+\gamma_7*P_{6,t}$
$(B_{8,t})=a_8*P_{7,t}+\gamma_8*P_{2,t}$

Star Wars IV -G16B1-QP=10		
	α	γ
B-1	0,302761	-1,00121
B-2	0,000524	0,270283
B-3	0,146268	0,10292
B-4	0,035253	0,220692
B-5	0,085625	0,166957
B-6	0,108868	0,140091
B-7	0,108641	0,141328
B-8	0,051458	0,215985

Star Wars IV-G16B1-QP=28

$(B_{1,t})=a_1*P_{1,t}+\gamma_1*B_{8,t-1}$
$(B_{2,t})=a_2*P_{2,t}+\gamma_2*B_{1,t}$
$(B_{3,t})=a_3*P_{3,t}+\gamma_3*B_{2,t}$
$(B_{4,t})=a_4*P_{4,t}+\gamma_4*B_{3,t}$
$(B_{5,t})=a_5*P_{5,t}+\gamma_5*B_{4,t}$
$(B_{6,t})=a_6*P_{6,t}+\gamma_6*B_{5,t}$
$(B_{7,t})=a_7*P_{7,t}+\gamma_7*B_{6,t}$
$(B_{8,t})=a_8*B_{6,t}+\gamma_8*B_{7,t}$

Star Wars IV -G16B1-QP=28		
	α	γ
B-1	0,045589	0,914731
B-2	0,087444	0,642946
B-3	0,060112	0,929012
B-4	0,046889	0,915059
B-5	0,039623	1,048782
B-6	0,050827	0,893891
B-7	0,069036	0,793765
B-8	0,829097	0,303841

Star Wars IV-G16B1-QP=48

$(B_{1,t})=a_1*P_{1,t}+\gamma_1*B_{8,t-1}$
$(B_{2,t})=a_2*P_{2,t}+\gamma_2*B_{1,t}$
$(B_{3,t})=a_3*P_{3,t}+\gamma_3*B_{2,t}$
$(B_{4,t})=a_4*P_{4,t}+\gamma_4*B_{3,t}$
$(B_{5,t})=a_5*P_{5,t}+\gamma_5*B_{4,t}$
$(B_{6,t})=a_6*P_{6,t}+\gamma_6*B_{5,t}$
$(B_{7,t})=a_7*P_{7,t}+\gamma_7*B_{6,t}$
$(B_{8,t})=a_8*B_{6,t}+\gamma_8*B_{7,t}$

Star Wars IV-G16B1-QP=48		
	α	γ
B-1	0,071483	0,814104
B-2	0,054215	0,861122
B-3	0,071956	0,792655
B-4	0,057554	0,83986
B-5	0,056859	0,839772
B-6	0,0662	0,810807
B-7	0,062052	0,829956
B-8	0,128026	0,94678

Star Wars IV-G16B3-QP=10

$$\widehat{B}_{1,t} = a_1 B_{11,t-1} + \gamma_1 B_{12,t-1}$$
$$\widehat{B}_{2,t} = a_2 B_{12,t-1} + \gamma_2 B_{1,t-1}$$
$$\widehat{B}_{3,t} = a_3 B_{1,t} + \gamma_3 B_{2,t}$$
$$\widehat{B}_{4,t} = a_4 B_{2,t} + \gamma_4 B_{3,t}$$
$$\widehat{B}_{5,t} = a_5 B_{3,t} + \gamma_5 B_{4,t}$$
$$\widehat{B}_{6,t} = a_6 B_{4,t} + \gamma_6 B_{5,t}$$
$$\widehat{B}_{7,t} = a_7 B_{5,t} + \gamma_7 B_{6,t}$$
$$\widehat{B}_{8,t} = a_8 B_{6,t} + \gamma_8 B_{7,t}$$
$$\widehat{B}_{9,t} = a_9 B_{7,t} + \gamma_9 B_{8,t}$$
$$\widehat{B}_{10,t} = a_{10} B_{8,t} + \gamma_{10} B_{9,t}$$
$$\widehat{B}_{11,t} = a_{11} B_{9,t} + \gamma_{11} B_{10,t}$$
$$\widehat{B}_{12,t} = a_{12} B_{10,t} + \gamma_{12} B_{11,t}$$

Star Wars IV -G16B3-QP=10		
	α	γ
B-1	0,990649	0,154828
B-2	0,966987	0,358207
B-3	0,105641	0,856314
B-4	0,966329	0,729002
B-5	0,960603	0,081054
B-6	0,227202	0,721576
B-7	0,974034	0,405562
B-8	1,039144	-0,12039
B-9	0,064857	0,837264
B-10	1,022473	0,013752
B-11	0,967071	-0,0274
B-12	0,276812	0,659793

Star Wars IV-G16B3-QP=28

$(B_{1,t})=a_1*B_{11,t-1}+\gamma_1*B_{12,t-1}$
$(B_{2,t})=a_2*B_{12,t-1}+\gamma_2*B_{1,t}$
$(B_{3,t})=a_3*B_{1,t}+\gamma_3*B_{2,t}$
$(B_{4,t})=a_4*B_{2,t}+\gamma_4*B_{3,t}$
$(B_{5,t})=a_5*B_{3,t}+\gamma_5*B_{4,t}$
$(B_{6,t})=a_6*B_{4,t}+\gamma_6*B_{5,t}$
$(B_{7,t})=a_7*B_{5,t}+\gamma_7*B_{6,t}$
$(B_{8,t})=a_8*B_{6,t}+\gamma_8*B_{7,t}$
$(B_{9,t})=a_9*B_{7,t}+\gamma_9*B_{8,t}$
$(B_{10,t})=a_{10}*B_{8,t}+\gamma_{10}*B_{9,t}$
$(B_{11,t})=a_{11}*B_{9,t}+\gamma_{11}*B_{10,t}$
$(B_{12,t})=a_{12}*B_{10,t}+\gamma_{12}*B_{11,t}$

Star Wars IV -G16B3-QP=28		
	α	γ
B-1	0,910919	0,043863
B-2	0,89066	0,1953
B-3	0,608791	0,423804
B-4	1,005886	0,052553
B-5	0,734	0,383577
B-6	0,447782	0,524786
B-7	0,918114	0,079129
B-8	0,848007	0,274098
B-9	0,321451	0,644675
B-10	0,966351	0,083704
B-11	0,814093	0,280107
B-12	0,064946	0,89039

Star Wars IV-G16B3-QP=48

$(B_{1,t})=a_1*B_{11,t-1}+\gamma_1*B_{12,t-1}$
$(B_{2,t})=a_2*B_{12,t-1}+\gamma_2*B_{1,t}$
$(B_{3,t})=a_3*B_{2,t}+\gamma_3*P_{1,t}$
$(B_{4,t})=a_4*B_{3,t}+\gamma_4*P_{2,t}$
$(B_{5,t})=a_5*B_{4,t}+\gamma_5* P_{2,t}$
$(B_{6,t})=a_6*B_{5,t}+\gamma_6* P_{2,t}$
$(B_{7,t})=a_7*B_{6,t}+\gamma_7* P_{3,t}$
$(B_{8,t})=a_8*B_{7,t}+\gamma_8* P_{3,t}$
$(B_{9,t})=a_9*B_{8,t}+\gamma_9* P_{3,t}$
$(B_{10,t})=a_{10}*B_{8,t}+\gamma_{10}*B_{9,t}$
$(B_{11,t})=a_{11}*B_{9,t}+\gamma_{11}*B_{10,t}$
$(B_{12,t})=a_{12}*B_{10,t}+\gamma_{12}*B_{11,t}$

Star Wars IV -G16B3-QP=48		
	α	γ
B-1	0,090428	0,963384
B-2	0,066159	0,943504
B-3	0,97214	0,010198
B-4	0,945952	0,013987
B-5	0,987247	0,006549
B-6	0,98747	0,003126
B-7	0,932703	0,016912
B-8	0,98404	0,008221
B-9	0,983897	0,004161
B-10	0,333226	0,746545
B-11	0,020938	0,990524
B-12	0,140911	0,862251

Star Wars IV-G16B7-QP=10

$(B_{1,t})=a_{1}*B_{11,t-1}+\gamma_{1}*B_{12,t-1}$

$(B_{2,t})=a_{2}*B_{12,t-1}+\gamma_{2}*B_{1,t}$

$(B_{3,t})=a_{3}*B_{1,t}+\gamma_{3}*B_{2,t}$

$(B_{4,t})=a_{4}*B_{2,t}+\gamma_{4}*B_{3,t}$

$(B_{5,t})=a_{5}*B_{3,t}+\gamma_{5}*B_{4,t}$

$(B_{6,t})=a_{6}*B_{4,t}+\gamma_{6}*B_{5,t}$

$(B_{7,t})=a_{7}*B_{5,t}+\gamma_{7}*B_{6,t}$

$(B_{8,t})=a_{8}*B_{6,t}+\gamma_{8}*B_{7,t}$

$(B_{9,t})=a_{9}*B_{7,t}+\gamma_{9}*B_{8,t}$

$(B_{10,t})=a_{10}*B_{8,t}+\gamma_{10}*B_{9,t}$

$(B_{11,t})=a_{11}*B_{9,t}+\gamma_{11}*B_{10,t}$

$(B_{12,t})=a_{12}*B_{10,t}+\gamma_{12}*B_{11,t}$

$(B_{13,t})=a_{13}*B_{11,t}+\gamma_{13}*B_{12,t}$

$(B_{14,t})=a_{14}*B_{12,t}+\gamma_{14}*B_{13,t}$

Star Wars IV -G16B7-QP=10		
	α	**γ**
B-1	0,971172	-0,22217
B-2	0,980892	0,575683
B-3	-0,50264	1,56255
B-4	0,537291	0,778753
B-5	0,146669	0,893102
B-6	-0,01387	0,933943
B-7	-0,01025	0,782554
B-8	0,945486	0,149044
B-9	1,034052	0,182883
B-10	-0,13496	1,235721
B-11	0,063171	0,969808
B-12	-0,00343	1,001308
B-13	0,007042	0,902964
B-14	-0,0241	0,776839

Star Wars IV-G16B7-QP=28

$(B_{1,t})=a_{1}*B_{11,t-1}+\gamma_{1}*B_{12,t-1}$

$(B_{2,t})=a_{2}*B_{12,t-1}+\gamma_{2}*B_{1,t}$

$(B_{3,t})=a_{3}*B_{1,t}+\gamma_{3}*B_{2,t}$

$(B_{4,t})=a_{4}*B_{2,t}+\gamma_{4}*B_{3,t}$

$(B_{5,t})=a_{5}*B_{3,t}+\gamma_{5}*B_{4,t}$

$(B_{6,t})=a_{6}*B_{4,t}+\gamma_{6}*B_{5,t}$

$(B_{7,t})=a_{7}*B_{5,t}+\gamma_{7}*B_{6,t}$

$(B_{8,t})=a_{8}*B_{6,t}+\gamma_{8}*B_{7,t}$

$(B_{9,t})=a_{9}*B_{7,t}+\gamma_{9}*B_{8,t}$

$(B_{10,t})=a_{10}*B_{8,t}+\gamma_{10}*B_{9,t}$

$(B_{11,t})=a_{11}*B_{9,t}+\gamma_{11}*B_{10,t}$

$(B_{12,t})=a_{12}*B_{10,t}+\gamma_{12}*B_{11,t}$

$(B_{13,t})=a_{13}*B_{11,t}+\gamma_{13}*B_{12,t}$

$(B_{14,t})=a_{14}*B_{12,t}+\gamma_{14}*B_{13,t}$

Star Wars IV -G16B7-QP=28		
	α	**γ**
B-1	0,825558	-0,04597
B-2	0,924532	0,392139
B-3	0,336602	0,991158
B-4	0,085875	1,052401
B-5	0,453867	0,574499
B-6	0,105249	0,800862
B-7	0,015807	0,763932
B-8	0,817198	0,023857
B-9	0,891359	0,489717
B-10	0,097555	1,127619
B-11	0,049587	1,017635
B-12	0,08303	0,928301
B-13	0,056563	0,852085
B-14	0,017932	0,77015

Star Wars IV-G16B7-QP=48

$(B_{1,t})=a_1*B_{11,t-1}+\gamma_1*B_{12,t-1}$
$(B_{2,t})=a_2*B_{12,t-1}+\gamma_2*B_{1,t}$
$(B_{3,t})=a_3*B_{1,t}+\gamma_3*B_{2,t}$
$(B_{4,t})=a_4*B_{2,t}+\gamma_4*B_{3,t}$
$(B_{5,t})=a_5*B_{3,t}+\gamma_5*B_{4,t}$
$(B_{6,t})=a_6*B_{4,t}+\gamma_6*B_{5,t}$
$(B_{7,t})=a_7*B_{5,t}+\gamma_7*B_{6,t}$
$(B_{8,t})=a_8*B_{6,t}+\gamma_8*B_{7,t}$
$(B_{9,t})=a_9*B_{7,t}+\gamma_9*B_{8,t}$
$(B_{10,t})=a_{10}*B_{8,t}+\gamma_{10}*B_{9,t}$
$(B_{11,t})=a_{11}*B_{9,t}+\gamma_{11}*B_{10,t}$
$(B_{12,t})=a_{12}*B_{10,t}+\gamma_{12}*B_{11,t}$
$(B_{13,t})=a_{13}*B_{11,t}+\gamma_{13}*B_{12,t}$
$(B_{14,t})=a_{14}*B_{12,t}+\gamma_{14}*B_{13,t}$

Star Wars IV -G16B7-QP=48		
	α	γ
B-1	0,120303	0,938284
B-2	0,031245	1,000114
B-3	0,058183	0,960913
B-4	0,043194	0,976615
B-5	0,125472	0,877188
B-6	0,122354	0,869314
B-7	0,071946	0,919135
B-8	0,189072	0,894161
B-9	0,019762	1,011804
B-10	-0,01347	1,030968
B-11	0,196081	0,823633
B-12	0,345172	0,660196
B-13	0,078984	0,91547
B-14	0,016243	0,973765

Star Wars IV-G16B15-QP=10

$(B_{1,t})=a_1*B_{11,t-1}+\gamma_1*B_{12,t-1}$
$(B_{2,t})=a_2*B_{12,t-1}+\gamma_2*B_{1,t}$
$(B_{3,t})=a_3*B_{1,t}+\gamma_3*B_{2,t}$
$(B_{4,t})=a_4*B_{2,t}+\gamma_4*B_{3,t}$
$(B_{5,t})=a_5*B_{3,t}+\gamma_5*B_{4,t}$
$(B_{6,t})=a_6*B_{4,t}+\gamma_6*B_{5,t}$
$(B_{7,t})=a_7*B_{5,t}+\gamma_7*B_{6,t}$
$(B_{8,t})=a_8*B_{6,t}+\gamma_8*B_{7,t}$
$(B_{9,t})=a_9*B_{7,t}+\gamma_9*B_{8,t}$
$(B_{10,t})=a_{10}*B_{8,t}+\gamma_{10}*B_{9,t}$
$(B_{11,t})=a_{11}*B_{9,t}+\gamma_{11}*B_{10,t}$
$(B_{12,t})=a_{12}*B_{10,t}+\gamma_{12}*B_{11,t}$
$(B_{13,t})=a_{13}*B_{11,t}+\gamma_{13}*B_{12,t}$
$(B_{14,t})=a_{14}*B_{12,t}+\gamma_{14}*B_{13,t}$
$(B_{15,t})=a_{15}*B_{13,t}+\gamma_{15}*B_{14,t}$

Star Wars IV -G16B15-QP=10		
	α	γ
B-1	0,974036	-0,31346
B-2	0,969232	0,726036
B-3	-0,61281	1,718496
B-4	1,427016	0,217368
B-5	1,150166	0,108871
B-6	-0,05444	1,101532
B-7	0,039118	0,995234
B-8	0,384605	0,661016
B-9	0,306999	0,75708
B-10	-0,01173	1,008773
B-11	0,042771	0,932155
B-12	0,004226	0,93795
B-13	0,008337	0,90306
B-14	-0,0189	0,867154
B-15	-0,00074	0,712847

Star Wars IV-G16B15-QP=28

$(B_{1,t})=a_{1}*B_{11,t-1}+\gamma_{1}*B_{12,t-1}$
$(B_{2,t})=a_{2}*B_{12,t-1}+\gamma_{2}*B_{1,t}$
$(B_{3,t})=a_{3}*B_{1,t}+\gamma_{3}*B_{2,t}$
$(B_{4,t})=a_{4}*B_{2,t}+\gamma_{4}*B_{3,t}$
$(B_{5,t})=a_{5}*B_{3,t}+\gamma_{5}*B_{4,t}$
$(B_{6,t})=a_{6}*B_{4,t}+\gamma_{6}*B_{5,t}$
$(B_{7,t})=a_{7}*B_{5,t}+\gamma_{7}*B_{6,t}$
$(B_{8,t})=a_{8}*B_{6,t}+\gamma_{8}*B_{7,t}$
$(B_{9,t})=a_{9}*B_{7,t}+\gamma_{9}*B_{8,t}$
$(B_{10,t})=a_{10}*B_{8,t}+\gamma_{10}*B_{9,t}$
$(B_{11,t})=a_{11}*B_{9,t}+\gamma_{11}*B_{10,t}$
$(B_{12,t})=a_{12}*B_{10,t}+\gamma_{12}*B_{11,t}$
$(B_{13,t})=a_{13}*B_{11,t}+\gamma_{13}*B_{12,t}$
$(B_{14,t})=a_{14}*B_{12,t}+\gamma_{14}*B_{13,t}$
$(B_{15,t})=a_{15}*B_{13,t}+\gamma_{15}*B_{14,t}$

Star Wars IV -G16B15-QP=28		
	α	**γ**
B-1	0,769798	-0,01078
B-2	0,886716	0,539872
B-3	0,351956	1,159373
B-4	0,080681	1,194394
B-5	0,666633	0,553447
B-6	0,18191	0,90473
B-7	0,072872	1,000552
B-8	0,338866	0,700622
B-9	0,100178	0,922212
B-10	0,063548	0,931265
B-11	0,062	0,926182
B-12	0,003343	0,934872
B-13	0,044572	0,862272
B-14	0,01204	0,83172
B-15	0,033077	0,70179

Star Wars IV-G16B15-QP=48

$(B_{1,t})=a_{1}*B_{11,t-1}+\gamma_{1}*B_{12,t-1}$
$(B_{2,t})=a_{2}*B_{12,t-1}+\gamma_{2}*B_{1,t}$
$(B_{3,t})=a_{3}*B_{1,t}+\gamma_{3}*B_{2,t}$
$(B_{4,t})=a_{4}*B_{2,t}+\gamma_{4}*B_{3,t}$
$(B_{5,t})=a_{5}*B_{3,t}+\gamma_{5}*B_{4,t}$
$(B_{6,t})=a_{6}*B_{4,t}+\gamma_{6}*B_{5,t}$
$(B_{7,t})=a_{7}*B_{5,t}+\gamma_{7}*B_{6,t}$
$(B_{8,t})=a_{8}*B_{6,t}+\gamma_{8}*B_{7,t}$
$(B_{9,t})=a_{9}*B_{7,t}+\gamma_{9}*B_{8,t}$
$(B_{10,t})=a_{10}*B_{8,t}+\gamma_{10}*B_{9,t}$
$(B_{11,t})=a_{11}*B_{9,t}+\gamma_{11}*B_{10,t}$
$(B_{12,t})=a_{12}*B_{10,t}+\gamma_{12}*B_{11,t}$
$(B_{13,t})=a_{13}*B_{11,t}+\gamma_{13}*B_{12,t}$
$(B_{14,t})=a_{14}*B_{12,t}+\gamma_{14}*B_{13,t}$
$(B_{15,t})=a_{15}*B_{13,t}+\gamma_{15}*B_{14,t}$

Star Wars IV -G16B15-QP=48		
	α	**γ**
B-1	0,17521	0,907538
B-2	0,038008	1,01652
B-3	-0,13959	1,171102
B-4	0,00469	1,034041
B-5	0,076168	0,952009
B-6	0,194602	0,827798
B-7	0,09229	0,920326
B-8	0,117692	0,891319
B-9	0,130893	0,871118
B-10	0,044567	0,953091
B-11	0,128395	0,866704
B-12	0,025959	0,969312
B-13	0,162986	0,823644
B-14	0.000097	0,983081
B-15	-0,01493	0,990449

Silence of the lambs-G16B1-QP=10

$(B_{1,t})=a_1*P_{1,t}+\gamma_1*P_{4,t}$
$(B_{2,t})=a_2*P_{2,t}+\gamma_2*P_{5,t}$
$(B_{3,t})=a_3*P_{3,t}+\gamma_3*P_{6,t}$
$(B_{4,t})=a_4*P_{4,t}+\gamma_4*P_{1,t}$
$(B_{5,t})=a_5*P_{5,t}+\gamma_5*P_{2,t}$
$(B_{6,t})=a_6*P_{6,t}+\gamma_6*P_{3,t}$
$(B_{7,t})=a_7*P_{7,t}+\gamma_7*P_{4,t}$
$(B_{8,t})=a_8*P_{5,t}+\gamma_8*P_{3,t}$

Silence of the Lambs -G16B1-QP=10		
	α	**γ**
B-1	0,207393	-0,01339
B-2	0,030884	0,164316
B-3	0,15095	0,036438
B-4	0,062841	0,136246
B-5	0,064009	0,133795
B-6	0,115947	0,072768
B-7	0,049843	0,144585
B-8	0,441481	-0,24179

Silence of the lambs-G16B1-QP=28

$(B_{1,t})=a_1*P_{1,t}+\gamma_1*P_{6,t}$
$(B_{2,t})=a_2*P_{2,t}+\gamma_2*P_{5,t}$
$(B_{3,t})=a_3*P_{3,t}+\gamma_3*P_{6,t}$
$(B_{4,t})=a_4*P_{4,t}+\gamma_4*P_{1,t}$
$(B_{5,t})=a_5*P_{5,t}+\gamma_5*P_{3,t}$
$(B_{6,t})=a_6*P_{6,t}+\gamma_6*P_{1,t}$
$(B_{7,t})=a_7*P_{2,t}+\gamma_7*P_{7,t}$
$(B_{8,t})=a_8*P_{3,t}+\gamma_8*P_{5,t}$

Silence of the Lambs-G16B1-QP=28		
	α	**γ**
B-1	0,078309	0,593091
B-2	0,026767	0,140564
B-3	0,025562	0,141268
B-4	0,0422	0,120079
B-5	0,041386	0,133564
B-6	0,033676	0,137866
B-7	0,008525	0,146116
B-8	0,008952	0,161506

Silence of the lambs-G16B1-QP=48

$(B_{1,t})=a_1*P_{1,t}+\gamma_1*B_{8,t-1}$
$(B_{2,t})=a_2*P_{2,t}+\gamma_2*B_{1,t}$
$(B_{3,t})=a_3*P_{3,t}+\gamma_3*B_{2,t}$
$(B_{4,t})=a_4*P_{4,t}+\gamma_4*B_{3,t}$
$(B_{5,t})=a_5*P_{5,t}+\gamma_5*B_{4,t}$
$(B_{6,t})=a_6*P_{6,t}+\gamma_6*B_{5,t}$
$(B_{7,t})=a_7*P_{7,t}+\gamma_7*B_{6,t}$
$(B_{8,t})=a_8*B_{6,t}+\gamma_8*B_{7,t}$

Silence of the Lambs -G16B1-QP=48		
	α	γ
B-1	0,035129	0,906945
B-2	0,030621	0,925038
B-3	0,033662	0,91495
B-4	0,028303	0,932151
B-5	0,031961	0,919542
B-6	0,02867	0,931547
B-7	0,032706	0,917821
B-8	0,273396	0,746946

Silence of the lambs-G16B3-QP=10

$(B_{1,t})=a_1*P_{1,t}+\gamma_1*P_{2,t}$
$(B_{2,t})=a_2*P_{1,t}+\gamma_2*P_{2,t}$
$(B_{3,t})=a_3*P_{1,t}+\gamma_3*P_{2,t}$
$(B_{4,t})=a_4*P_{2,t}+\gamma_4*P_{3,t}$
$(B_{5,t})=a_5*P_{2,t}+\gamma_5*P_{1,t}$
$(B_{6,t})=a_6*P_{2,t}+\gamma_6*P_{1,t}$
$(B_{7,t})=a_7*P_{3,t}+\gamma_7*P_{1,t}$
$(B_{8,t})=a_8*P_{3,t}+\gamma_8*P_{2,t}$
$(B_{9,t})=a_9*P_{3,t}+\gamma_9*P_{2,t}$
$(B_{10,t})=a_{10}*P_{2,t}+\gamma_{10}*P_{1,t}$
$(B_{11,t})=a_{11}*P_{3,t}+\gamma_{11}*P_{2,t}$
$(B_{12,t})=a_{12}*P_{3,t}+\gamma_{12}*P_{1,t}$

Silence of the Lambs -G16B3-QP=10		
	α	γ
B-1	0,191536	0,058326
B-2	0,205266	0,110768
B-3	0,213629	0,044942
B-4	0,156577	0,095701
B-5	0,04798	0,280695
B-6	0,069486	0,193862
B-7	0,144673	0,105046
B-8	0,121556	0,199197
B-9	0,126901	0,12751
B-10	1,045723	-0,84319
B-11	0,10425	0,223243
B-12	0,49673	-0,19673

Silence of the lambs-G16B3-QP=28

$(B_{1,t})=a_1*B_{11,t-1}+\gamma_1*B_{12,t-1}$
$(B_{2,t})=a_2*P_{1,t}+\gamma_2*P_{2,t}$
$(B_{3,t})=a_3*B_{2,t}+\gamma_3*P_{1,t}$
$(B_{4,t})=a_4*B_{2,t}+\gamma_4*B_{3,t}$
$(B_{5,t})=a_5*P_{2,t}+\gamma_5*P_{1,t}$
$(B_{6,t})=a_6*B_{5,t}+\gamma_6*P_{2,t}$
$(B_{7,t})=a_7*B_{6,t}+\gamma_7*P_{3,t}$
$(B_{8,t})=a_8*P_{3,t}+\gamma_8*P_{2,t}$
$(B_{9,t})=a_9*B_{7,t}+\gamma_9*B_{8,t}$
$(B_{10,t})=a_{10}*B_{8,t}+\gamma_{10}*B_{9,t}$
$(B_{11,t})=a_{11}*P_{3,t}+\gamma_{11}*P_{2,t}$
$(B_{12,t})=a_{12}*B_{10,t}+\gamma_{12}*B_{11,t}$

Silence of the Lambs -G16B3-QP=28		
	α	**γ**
B-1	0,995582	-0,01673
B-2	0,029662	0,168565
B-3	0,772131	0,020552
B-4	0,960963	0,232255
B-5	0,032512	0,16439
B-6	0,774882	0,020503
B-7	0,452803	0,085373
B-8	0,026672	0,176402
B-9	0,181057	0,768819
B-10	1,042371	-0,02207
B-11	0,070297	0,136242
B-12	0,288678	0,669292

Silence of the lambs-G16B3-QP=48

$(B_{1,t})=a_1*B_{11,t-1}+\gamma_1*B_{12,t-1}$
$(B_{2,t})=a_2*B_{12,t-1}+\gamma_2*B_{1,t}$
$(B_{3,t})=a_3*B_{1,t}+\gamma_3*B_{2,t}$
$(B_{4,t})=a_4*B_{2,t}+\gamma_4*B_{3,t}$
$(B_{5,t})=a_5*B_{3,t}+\gamma_5*B_{4,t}$
$(B_{6,t})=a_6*B_{4,t}+\gamma_6*B_{5,t}$
$(B_{7,t})=a_7*B_{5,t}+\gamma_7*B_{6,t}$
$(B_{8,t})=a_8*B_{6,t}+\gamma_8*B_{7,t}$
$(B_{9,t})=a_9*B_{7,t}+\gamma_9*B_{8,t}$
$(B_{10,t})=a_{10}*B_{8,t}+\gamma_{10}*B_{9,t}$
$(B_{11,t})=a_{11}*B_{9,t}+\gamma_{11}*B_{10,t}$
$(B_{12,t})=a_{12}*B_{10,t}+\gamma_{12}*B_{11,t}$

Silence of the Lambs -G16B3-QP=48		
	α	**γ**
B-1	0,563097	0,451061
B-2	0,101082	0,912576
B-3	0,291525	0,710842
B-4	0,365687	0,661543
B-5	0,164539	0,843991
B-6	0,200891	0,800706
B-7	0,500084	0,526005
B-8	0,0662	0,944271
B-9	0,208096	0,798243
B-10	0,265156	0,78065
B-11	0,071885	0,934197
B-12	0,242887	0,751574

Silence of the lambs-G16B7-QP=10

$(B_{1,t})=a_1*B_{13,t-1}+\gamma_1*B_{14,t-1}$
$(B_{2,t})=a_2*P_{1,t-1}+\gamma_2*B_{1,t}$
$(B_{3,t})=a_3*P_{1,t}+\gamma_3*B_{2,t}$
$(B_{4,t})=a_4*P_{1,t}+\gamma_4*B_{3,t}$
$(B_{5,t})=a_5*P_{1,t}+\gamma_5*B_{4,t}$
$(B_{6,t})=a_6*P_{1,t}+\gamma_6*B_{5,t}$
$(B_{7,t})=a_7*B_{5,t}+\gamma_7*B_{6,t}$
$(B_{8,t})=a_8*B_{6,t}+\gamma_8*B_{7,t}$
$(B_{9,t})=a_9*B_{8,t}+\gamma_9*P_{1,t}$
$(B_{10,t})=a_{10}*P_{1,t}+\gamma_{10}*B_{9,t}$
$(B_{11,t})=a_{11}*P_{1,t}+\gamma_{11}*B_{10,t}$
$(B_{12,t})=a_{12}*B_{11,t}+\gamma_{12}*P_{1,t}$
$(B_{13,t})=a_{13}*B_{12,t}+\gamma_{13}*P_{1,t}$
$(B_{14,t})=a_{14}*B_{12,t}+\gamma_{14}*B_{13,t}$

Silence of the Lambs -G16B7-QP=10		
	α	γ
B-1	0,994131	0,719739
B-2	0,397142	-8,42423
B-3	0,029092	1,023853
B-4	0,011949	1,006573
B-5	0,030757	0,900129
B-6	0,004304	0,909247
B-7	-0,01059	0,717334
B-8	0,99139	0,3722
B-9	0,665345	0,173029
B-10	0,013642	1,050924
B-11	0,003353	1,016096
B-12	1,002367	-0,00698
B-13	1,232202	-0,1106
B-14	-0,00825	0,698857

Silence of the lambs-G16B7-QP=28

$(B_{1,t})=a_1*B_{11,t-1}+\gamma_1*B_{12,t-1}$
$(B_{2,t})=a_2*B_{12,t-1}+\gamma_2*B_{1,t}$
$(B_{3,t})=a_3*B_{1,t}+\gamma_3*B_{2,t}$
$(B_{4,t})=a_4*B_{2,t}+\gamma_4*B_{3,t}$
$(B_{5,t})=a_5*B_{3,t}+\gamma_5*B_{4,t}$
$(B_{6,t})=a_6*B_{4,t}+\gamma_6*B_{5,t}$
$(B_{7,t})=a_7*B_{5,t}+\gamma_7*B_{6,t}$
$(B_{8,t})=a_8*B_{6,t}+\gamma_8*B_{7,t}$
$(B_{9,t})=a_9*B_{7,t}+\gamma_9*B_{8,t}$
$(B_{10,t})=a_{10}*B_{8,t}+\gamma_{10}*B_{9,t}$
$(B_{11,t})=a_{11}*B_{9,t}+\gamma_{11}*B_{10,t}$
$(B_{12,t})=a_{12}*B_{10,t}+\gamma_{12}*B_{11,t}$
$(B_{13,t})=a_{13}*B_{11,t}+\gamma_{13}*B_{12,t}$
$(B_{14,t})=a_{14}*B_{12,t}+\gamma_{14}*B_{13,t}$

Silence of the Lambs -G16B7-QP=28		
	α	γ
B-1	0,967567	-0,26758
B-2	0,951775	0,284708
B-3	-0,15986	1,349092
B-4	0,057391	1,034048
B-5	0,068579	0,954667
B-6	0,008557	0,904874
B-7	0,067073	0,698855
B-8	1,003808	-0,33444
B-9	0,928549	0,429777
B-10	-0,17864	1,33233
B-11	0,029346	1,037912
B-12	0,090612	0,901272
B-13	-0,00348	0,92153
B-14	-0,11323	0,91294

Silence of the lambs-G16B7-QP=48

$(B_{1,t})=a_1*B_{11,t-1}+\gamma_1*B_{12,t-1}$
$(B_{2,t})=a_2*B_{12,t-1}+\gamma_2*B_{1,t}$
$(B_{3,t})=a_3*B_{1,t}+\gamma_3*B_{2,t}$
$(B_{4,t})=a_4*B_{2,t}+\gamma_4*B_{3,t}$
$(B_{5,t})=a_5*B_{3,t}+\gamma_5*B_{4,t}$
$(B_{6,t})=a_6*B_{4,t}+\gamma_6*B_{5,t}$
$(B_{7,t})=a_7*B_{5,t}+\gamma_7*B_{6,t}$
$(B_{8,t})=a_8*B_{6,t}+\gamma_8*B_{7,t}$
$(B_{9,t})=a_9*B_{7,t}+\gamma_9*B_{8,t}$
$(B_{10,t})=a_{10}*B_{8,t}+\gamma_{10}*B_{9,t}$
$(B_{11,t})=a_{11}*B_{9,t}+\gamma_{11}*B_{10,t}$
$(B_{12,t})=a_{12}*B_{10,t}+\gamma_{12}*B_{11,t}$
$(B_{13,t})=a_{13}*B_{11,t}+\gamma_{13}*B_{12,t}$
$(B_{14,t})=a_{14}*B_{12,t}+\gamma_{14}*B_{13,t}$

Silence of the Lambs -G16B7-QP=48		
	α	**γ**
B-1	0,381087	0,650732
B-2	0,202615	0,830541
B-3	0,040862	0,979909
B-4	0,073595	0,941474
B-5	0,188268	0,812398
B-6	0,182657	0,810041
B-7	0,017262	0,969577
B-8	0,305745	0,744184
B-9	0,079507	0,949583
B-10	0,096411	0,922471
B-11	0,075552	0,931363
B-12	0,067128	0,92993
B-13	0,1194	0,870015
B-14	0,002076	0,981067

Silence of the lambs-G16B15-QP=10

$(B_{1,t})=a_1*B_{11,t-1}+\gamma_1*B_{12,t-1}$
$(B_{2,t})=a_2*B_{12,t-1}+\gamma_2*B_{1,t}$
$(B_{3,t})=a_3*B_{1,t}+\gamma_3*B_{2,t}$
$(B_{4,t})=a_4*B_{2,t}+\gamma_4*B_{3,t}$
$(B_{5,t})=a_5*B_{3,t}+\gamma_5*B_{4,t}$
$(B_{6,t})=a_6*B_{4,t}+\gamma_6*B_{5,t}$
$(B_{7,t})=a_7*B_{5,t}+\gamma_7*B_{6,t}$
$(B_{8,t})=a_8*B_{6,t}+\gamma_8*B_{7,t}$
$(B_{9,t})=a_9*B_{7,t}+\gamma_9*B_{8,t}$
$(B_{10,t})=a_{10}*B_{8,t}+\gamma_{10}*B_{9,t}$
$(B_{11,t})=a_{11}*B_{9,t}+\gamma_{11}*B_{10,t}$
$(B_{12,t})=a_{12}*B_{10,t}+\gamma_{12}*B_{11,t}$
$(B_{13,t})=a_{13}*B_{11,t}+\gamma_{13}*B_{12,t}$
$(B_{14,t})=a_{14}*B_{12,t}+\gamma_{14}*B_{13,t}$
$(B_{15,t})=a_{15}*B_{13,t}+\gamma_{15}*B_{14,t}$

Silence of the Lambs -G16B15-QP=10		
	α	**γ**
B-1	0,989609	0,778145
B-2	0,982551	1,253596
B-3	-0,126	1,325664
B-4	-0,07228	1,174036
B-5	-0,0812	1,154814
B-6	-0,03356	1,074077
B-7	-0,00252	1,02978
B-8	-0,03714	1,049402
B-9	0,067686	0,939517
B-10	-0,02795	1,018523
B-11	-0,00252	0,974149
B-12	-0,00432	0,955293
B-13	0,082157	0,833798
B-14	-0,01761	0,881737
B-15	-0,00508	0,669496

Silence of the lambs-G16B15-QP=28

$(B_{1,t})=a_1*B_{11,t-1}+\gamma_1*B_{12,t-1}$
$(B_{2,t})=a_2*B_{12,t-1}+\gamma_2*B_{1,t}$
$(B_{3,t})=a_3*B_{1,t}+\gamma_3*B_{2,t}$
$(B_{4,t})=a_4*B_{2,t}+\gamma_4*B_{3,t}$
$(B_{5,t})=a_5*B_{3,t}+\gamma_5*B_{4,t}$
$(B_{6,t})=a_6*B_{4,t}+\gamma_6*B_{5,t}$
$(B_{7,t})=a_7*B_{5,t}+\gamma_7*B_{6,t}$
$(B_{8,t})=a_8*B_{6,t}+\gamma_8*B_{7,t}$
$(B_{9,t})=a_9*B_{7,t}+\gamma_9*B_{8,t}$
$(B_{10,t})=a_{10}*B_{8,t}+\gamma_{10}*B_{9,t}$
$(B_{11,t})=a_{11}*B_{9,t}+\gamma_{11}*B_{10,t}$
$(B_{12,t})=a_{12}*B_{10,t}+\gamma_{12}*B_{11,t}$
$(B_{13,t})=a_{13}*B_{11,t}+\gamma_{13}*B_{12,t}$
$(B_{14,t})=a_{14}*B_{12,t}+\gamma_{14}*B_{13,t}$
$(B_{15,t})=a_{15}*B_{13,t}+\gamma_{15}*B_{14,t}$

Silence of the Lambs -G16B15-QP=28		
	α	**γ**
B-1	-0,20133	1,48105
B-2	-0,08642	1,270926
B-3	-0,00611	1,149204
B-4	0,229537	0,896207
B-5	-0,02939	1,089717
B-6	0,222011	0,824521
B-7	0,06324	0,951073
B-8	0,085834	0,907015
B-9	0,0008	0,961824
B-10	0,016556	0,919312
B-11	-0,00741	0,904375
B-12	0,000782	0,83939
B-13	-0,02503	0,752071
B-14	0,967618	-0,38558
B-15	0,939108	0,374402

Silence of the lambs-G16B15-QP=48

$(B_{1,t})=a_1*B_{11,t-1}+\gamma_1*B_{12,t-1}$
$(B_{2,t})=a_2*B_{12,t-1}+\gamma_2*B_{1,t}$
$(B_{3,t})=a_3*B_{1,t}+\gamma_3*B_{2,t}$
$(B_{4,t})=a_4*B_{2,t}+\gamma_4*B_{3,t}$
$(B_{5,t})=a_5*B_{3,t}+\gamma_5*B_{4,t}$
$(B_{6,t})=a_6*B_{4,t}+\gamma_6*B_{5,t}$
$(B_{7,t})=a_7*B_{5,t}+\gamma_7*B_{6,t}$
$(B_{8,t})=a_8*B_{6,t}+\gamma_8*B_{7,t}$
$(B_{9,t})=a_9*B_{7,t}+\gamma_9*B_{8,t}$
$(B_{10,t})=a_{10}*B_{8,t}+\gamma_{10}*B_{9,t}$
$(B_{11,t})=a_{11}*B_{9,t}+\gamma_{11}*B_{10,t}$
$(B_{12,t})=a_{12}*B_{10,t}+\gamma_{12}*B_{11,t}$
$(B_{13,t})=a_{13}*B_{11,t}+\gamma_{13}*B_{12,t}$
$(B_{14,t})=a_{14}*B_{12,t}+\gamma_{14}*B_{13,t}$
$(B_{15,t})=a_{15}*B_{13,t}+\gamma_{15}*B_{14,t}$

Silence of the Lambs -G16B15-QP=48		
	α	**γ**
B-1	0,353561	0,707882
B-2	0,099652	0,947197
B-3	0,069322	0,971096
B-4	0,017734	1,011203
B-5	0,038621	0,979849
B-6	0,138277	0,881592
B-7	0,121183	0,888778
B-8	0,265956	0,744599
B-9	0,101457	0,902808
B-10	0,047768	0,949621
B-11	0,209558	0,781109
B-12	0,111224	0,87807
B-13	0,011573	0,970653
B-14	0,030393	0,949656
B-15	-0,02474	0,998761